AD-A008 403

I. NEW TECHNIQUES FOR THE SUNTHESIS OF METALS AND ALLOYS. II. THE PROPERTIES OF RARE EARTH METALS AND ALLOYS

R. F. Bunshah, et al

California University

Prepared for:

Advanced Research Projects Agency

November 1974

DISTRIBUTED BY:

NTIS

National Technical Information Service
U. S. DEPARTMENT OF COMMERCE

SECURITY CLASSIFICATION OF THIS PAGE (When Data Entered)

REPORT DOCUMENTATION PAGE		READ INSTRUCTIONS BEFORE COMPLETING FORM
1. REPORT NUMBER	2. GOVT ACCESSION NO.	3. RECIPIENT'S CATALOG NUMBER AD-A008 403
4. TITLE (and Subtitle) "New Techniques for the Synthesis of Metals and Alloys" "The Properties of Rare Earth Metals and Alloys"		5. TYPE OF REPORT & PERIOD COVERED Final Report July 1, 1970-June 30, 1974
		6. PERFORMING ORG. REPORT NUMBER UCLA-ENG-7520
7. AUTHOR(s) R. F. Bunshah D. L. Douglass		8. CONTRACT OR GRANT NUMBER(s) Grant No. DAHC 15-70-G-15 Order No. AO 1643
9. PERFORMING ORGANIZATION NAME AND ADDRESS School of Engineering and Applied Science University of California Los Angeles, California 90024		10. PROGRAM ELEMENT, PROJECT, TASK AREA & WORK UNIT NUMBERS
11. CONTROLLING OFFICE NAME AND ADDRESS Advanced Research Projects Agency Washington, D. C. 20301		12. REPORT DATE November 1974 13. NUMBER OF PAGES 78
14. MONITORING AGENCY NAME & ADDRESS(if different from Controlling Office)		15. SECURITY CLASS. (of this report) Unclassified 15a. DECLASSIFICATION/DOWNGRADING SCHEDULE

16. DISTRIBUTION STATEMENT (of this Report)

Approved for public release; distribution unlimited.

17. DISTRIBUTION STATEMENT (of the abstract entered in Block 20, if different from Report)

DDC
RECEIVED
APR 17 1975
D

18. SUPPLEMENTARY NOTES

Reproduced by
NATIONAL TECHNICAL
INFORMATION SERVICE
US Department of Commerce
Springfield, VA. 22151

19. KEY WORDS (Continue on reverse side if necessary and identify by block number) ***See back side for Cont.

Activated Reactive Evaporation
Carbides
Condensation
Deposit
Deposition Temperature
Evaporation Dispersion Strengthened Alloy
Evaporation Apparatus
Gas Scattering Evaporation
High Rate Physical Vapor Deposition Process
Hafnium Carbide ***

20. ABSTRACT (Continue on reverse side if necessary and identify by block number)

This investigation consisted of two parts. In part one, a High Rate Physical Vapor Deposition Process was developed for the deposition of metals, alloys, compounds and dispersion strengthened alloys. The relationship between the deposition temperature, the microstructure, and the mechanical properties was studied. The materials resulting from this process were shown to have properties very similar to true engineering materials. These deposition techniques have been developed to the stage where they can be applied to the pro-

DD FORM 1 JAN 73 1473 EDITION OF 1 NOV 65 IS OBSOLETE
S/N 0102-014-6601

SECURITY CLASSIFICATION OF THIS PAGE (When Data Entered)

duction of self-supporting shapes or coatings for engineering applications.

The second part of this investigation was concerned with the study of the oxidation mechanism of Ni_3Al containing yttrium.

19. (Continued)
Lattice Parameter
Microhardness
Nichrome
Ni_3Al
Nickel
Nickel - TiC Dispersion Strengthened Alloy
Nitrides
Oxidation
Oxides
Reactive Evaporation
Refractory Carbides
Silicon Nitride - Si_3N_4
Substrate
Synthesis of Materials
Temperature Distribution
Thickness Distribution
Titanium Carbide
Yttria - Y_2O_3
Yttrium
Zirconium Carbide

UCLA-ENG-7520
NOVEMBER 1974

FINAL REPORT

I. New Techniques for the Synthesis of Metals and Alloys
(Principal Investigator - Professor R.F. Bunshah)

II. The Properties of Rare Earth Metals and Alloys
(Principal Investigator - Professor D.L. Douglass)

Sponsor: The Advanced Research Projects Agency
Grant No.: DAHC 15-70-G-15
ARPA Order No.: AO 1643
Effective Date: July 1, 1970
Contract Expiration Date: June 30, 1973
Amount of Contract: $298,398
Classification: Unclassified

This research was sponsored by the Advanced Research Projects Agency of the Department of Defense under Contract No. DAHC 15-70-G-15

Materials Department
School of Engineering and Applied Science
University of California
Los Angeles, California

ABSTRACT

This investigation consisted of two parts. In part one, a High Rate Physical Vapor Deposition Process was developed for the deposition of metals, alloys, compounds and dispersion strengthened alloys. The relationship between the deposition temperature, the microstructure and the mechanical properties was studied. The materials resulting from this process were shown to have properties very similar to true engineering materials. These deposition techniques have been developed to the stage where they can be applied to the production of self-supporting shapes or coatings for engineering applications.

The second part of this investigation was concerned with the study of the oxidation mechanism of Ni_3Al continaing yttrium.

TABLE OF CONTENTS

Preceding page blank

LIST OF FIGURES

Preceding page blank

LIST OF TABLES

Preceding page blank

I. INTRODUCTION

This is the final report describing research activities on ARPA Grant No. DAHC 15-70-G-15. The scope of the work is divided into two major areas of effort and further subdivided into two major areas as shown below.

1. New Techniques for the Synthesis of Metals and Alloys (Professor R.F. Bunshah, Principal Investigator).
2. The Properties of Rare Earth Metals and Alloys (Professor D.L. Douglass, Principal Investigator).

II. NEW TECHNIQUES FOR THE SYNTHESIS OF METALS AND ALLOYS

A. Background

High Rate Physical Vapor Deposition (HRPVD) techniques[1-8] are to be used to prepare metallic alloys, ceramics, and metal-ceramic mixtures (dispersion strengthened alloys). The method consists of evaporation of metals, alloys and ceramics contained in water cooled crucibles using high power electron beams. The process is carried out in a high vacuum environment. The use of high power electron beams makes it possible to produce very high evaporation rates. The vapors are collected on heated metallic substrates to produce full density deposits at high deposition rates.

The HRPVD process has several advantages which make them unique, particularly since many of them can be obtained simultaneously. They are:

1. Production of simple shapes (sheet, foil, tubing) directly, of full density, from metals, alloys and ceramics at high deposition rates (.001" or 250,000 A/min), which is a very important economic consideration.

2. Very high purity of the deposits.

3. Very fine grain size (~1μ) in the deposits, thus increasing strength with toughness as contrasted to other methods of strengthening such as solid solution or precipitation, where strength is increased at the expense of toughness.

4. Excellent bonding to the substrate (a parting compound has to be used to separate the deposit from the substrate when it is desired to produce a self-supported shape like a sheet).

5. Surface finish equal to that of the substrate, thus minimizing or eliminating post-deposition machining or grinding.

High deposition rates on a sustained basis can only be obtained with a heat source which produces a high power density at the evaporant surface. Electron beam heated sources have been used very successfully for this purpose.[9] Evaporation rates from such sources obey an equation of the form of

$$R_V = CW^n$$

where W is the incident power of the electron beam, and n and C are constants that depend on coating material and evaporant geometry.[13] The exponent n can be as high as 8. Thus, even slight variations in electron beam power can cause large changes in evaporation rate. In those cases where deposition rate and coating thickness are important, the electron beam power is coupled to the output of a deposition rate monitor via a suitable feed-back circuit.

The evaporant is generally contained in water-cooled copper crucibles which are mandatory for the evaporation of reactive and refractory metals like Ti, Be, Mo, W, etc. since these would react with oxide crucibles. High rate evaporation of pure metals of high thermal conductivity

like Ag, Al, Au, Cu from water-cooled copper crucibles is difficult since a large fraction of the input power is lost to the crucible. In such cases, refractory liners of graphite, glassy carbon, BN, TiB_2-ZrB_2, etc., are often used to minimize the power losses to the water-cooled crucible. Figure 1 is a schematic of a batch-type evaporation system using electron beam heating. Continuous or semi-continuous coating systems using electron beam heating have been discussed in the literature.[10] In special cases, very high deposition rates have been obtained for aluminum using inductive heating sources and in the case of zinc, extremely high deposition rates have been obtained with resistance heated sources.[11]

It should be noted that the condensation temperature is a very important process variable. Bunshah and Juntz[8] found that for titanium, as the deposition temperature is lowered the grain size of the fully dense deposit becomes finer. At very low temperatures (~25% of the melting point) the deposit has less than full density. Since a fine grain sized microstructure represents an optimum condition of strength and toughness in a material, the importance of control of the deposition temperature becomes obvious.

This observation was systemized when Movchan and Demchishin[14] first proposed the following model which relates the deposit morphology to the deposition temperature. It is illustrated in Fig. 2. Three characteristic structural zones are formed in the condensates of pure substances by increasing the temperature of the surface on which condensation takes place. For low temperature zone, zone 1, the upper boundary equals ~$0.3T_m$, T_m being the melting point of the evaporated material; an

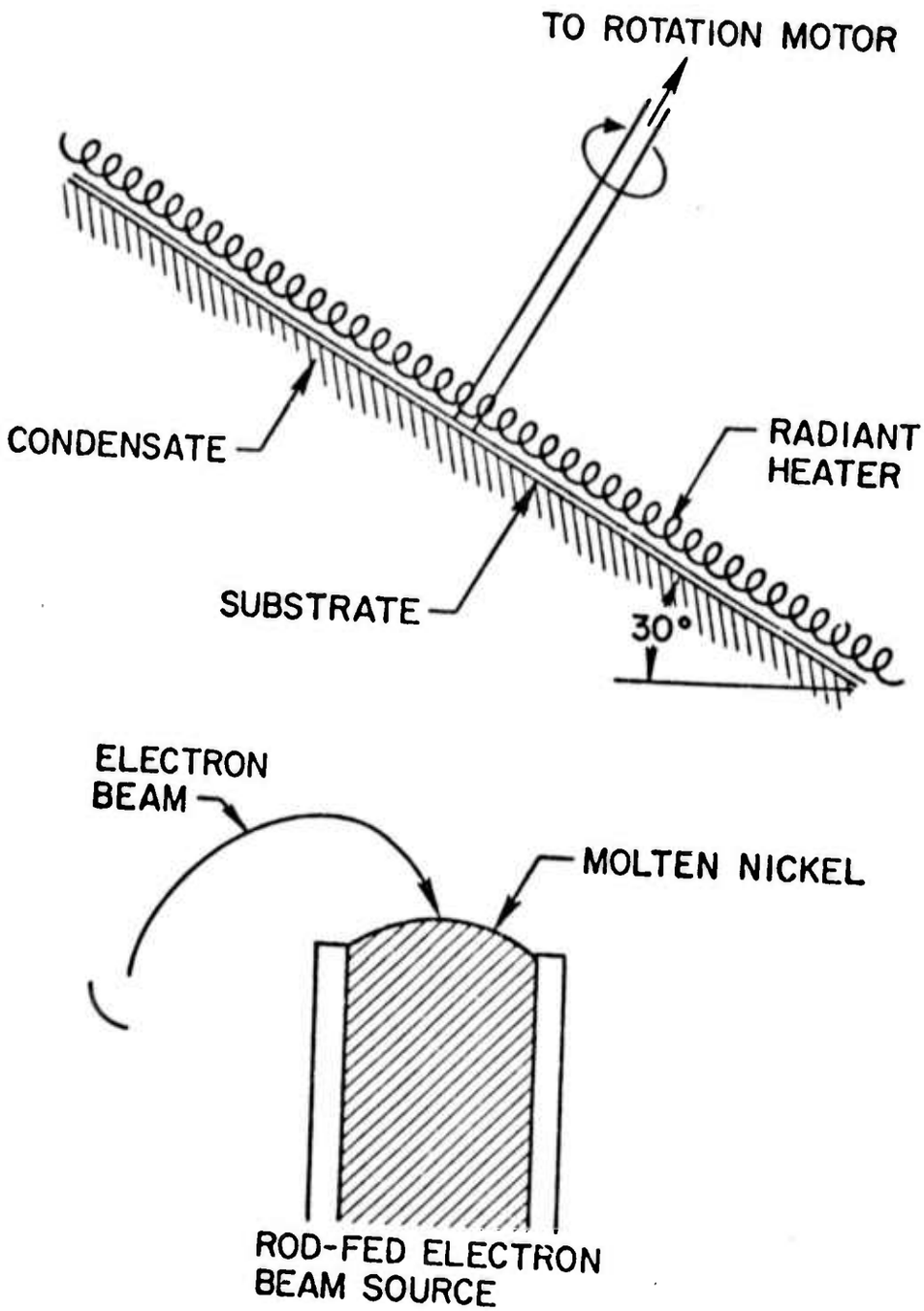

Figure 1. Schematic of Deposition Set-Up.

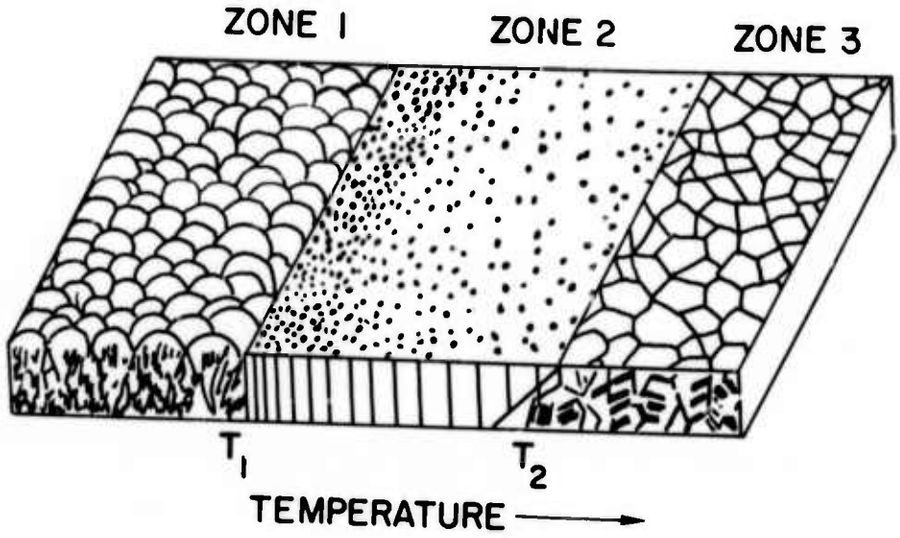

	ZONE 1	ZONE 2	ZONE 3
METALS	$<0.3\ T'_m$	$0.3 - 0.45\ T'_m$	$>0.45\ T'_m$
OXIDES	$<0.26\ T'_m$	$0.26 - 0.45\ T'_m$	$>0.45\ T'_m$

Figure 2. Structural Zones in Condensates at Various Substrate Temperatures (Movchan and Demchishin).

intermediate zone, zone 2, between 0.3 to 0.5 T_m; and a high temperature zone, zone 3, above 0.5 T_m evaporated substance. Each of these zones has its own features of structure and physical-chemical properties. For example, the condensates of pure metals, iron, nickel , titanium, tungsten have high hardness, low density and ductility in the low temperature zone 1. The properties of the intermediate temperature zone 2 approach those of the cast metals, the condensates also showing a typical columnar structure. The condensates in the high temperature zone 3 have an equiaxed structure, low hardness, high density and ductility, with properties approaching those of wrought and annealed metals. The above differences in structure and properties can be explained by the various thermal activation mechanisms controlling the formation of structures within each zone. In the low temperature zone, probably, the processes of surface diffusion are not taking place very vigorously; only the collision of growing three dimensional islands without sufficient development of coalescence occurs, and imperfections of the crystal lattice are chaotically distributed. As a result, the structure grows as tapered crystallites or cones. The surface shows a domed appearance and hence it has also been called Botroidal. It contains longitudinally oriented porosity of the order of a few hundred angstroms width between the tapered crystallites. Each crystallite consists of numerous sub-micron size grains. In the intermediate temperature zone 2, apparently, the processes of "surface recrystallization" take place resulting in the coalescence of differently oriented islands resulting in a more ordered surface with preferred orientation. It results in the columnar grains with clearly observed intercrystalline boundaries. The grain diameter increases with temperature. In the high temperature zone 3, the processes of volume diffusion are well developed. These mechanisms have been qualitatively

confirmed by transmission electron microscopy of thin nickel films prepared from massive nickel condensates. A high density of chaotically distributed dislocations and micropores are observed in the low temperature zone. In the intermediate temperature zone, a marked decrease of the number of line imperfections has taken place simultaneously with their rearrangement; dislocations are located primarily at the zone boundary and micropores are practically absent. The fine equiaxed structure in the high temperature zone is identical to that of a bulk metal equilibrium after annealing. The transition between the various zones is not sharp, i.e. at a definite temperature. Rather, the zones blend into one another.

An elegant proof of the importance of surface mobility was also provided by Movchan and Demchishin.[14] Plots of the log of the grain diameter vs. the inverse of deposition temperature in zones 2 and 3 yield straight lines from which activation energies can be computed. It was found that the activation energy for zone 2 growth corresponded to that for surface self-diffusion and for zone 3 growth to volume self-diffusion.

B. Scope of the Work

The objective of this portion of the research grant was to investigate the potential of synthesizing deposits of various types of materials using high rate physical vapor deposition techniques. Four types of materials, i.e., metals, alloys, ceramics and dispersion strengthened alloys were to be studied. Specific examples were chosen, e.g. the metal being represented by nickel, the alloy by Ni-20Cr, the ceramics by TiC, Y_2O_3 and Si_3N_4, and the dispersion strengthened alloys by Ni-TiC. The microstructure and properties of the deposit were varied by changing the

deposition temperature. These changes were studied as part of this investigation.

Very essential to the preparation of suitable test specimens are two other factors:

1. Design of the apparatus for high rate physical vapor deposition.
2. Theoretical calculation of the thickness distribution and temperature distribution of the deposited material which in this case is in the form of a sheet.

Both of these tasks are essential preliminaries to the main scope of work and are detailed below.

C. High Rate Physical Vapor Deposition Apparatus for Metals, Alloys, Dispersion Strengthened Alloys, and Ceramics

Such an apparatus is quite complex and has many state-of-the-art features. The requirements for such an apparatus are as follows:

1. High rate evaporation of metals, alloys or ceramics from one source or two sources simultaneously. Sources should be rod-fed to permit long time uniform evaporations.
2. Electron beam heating incorporated into the sources to get high evaporation rates. In addition, beam scanning of the source should be available in one of the sources which is used for the direct evaporation of ceramics or dielectrics.
3. Substrate holder capable of:

    a) Heating the substrate to an elevated temperature and controlling it at the desired temperature. This is necessary to produce a fully dense deposit. The apparatus will have capability of:-

        i) heating a 10" x 10" substrate up to 1000°C by radiant heating from the back.

ii) direct resistance heating of one or more 1/2" x 3" strips to 1500°C.

b) Rotation of the 10" x 10" substrate and the ability to tilt the axis of rotation up to 45° from the vertical. This is necessary to produce a uniform thickness of deposit over the entire substrate.

4. A high vacuum environment capable of maintaining a working pressure of 5.10^{-6} torr or lower and a base pressure of 2.10^{-7} torr or lower. The vacuum environment should be monitored using residual gas analyzers. The best vacuum techniques should be used to keep contamination of the deposit from back-streaming of oil vapors and from other sources to a minimum.

5. A liquid pool level monitor to keep the height of the liquid pool at the desired level. This is necessary to keep the alloy composition in the vapor phase at a constant value.

6. Capability to bleed gases or gas mixtures at the desired partial pressures in the vicinity of the substrates. This is necessary to carry out reactive evaporation processes effectively.

7. The ability to feed raw material and melt it into evaporant stock. This feature is very desirable as the raw material for evaporant stock should have very low gas content to avoid spattering of liquid droplets during evaporation. Not all evaporant materials can be purchased in the desired form. Rod fed electron beam sources also require the feed rod to have outside diameter to fit the inside diameter of the opening in the source after allowing for thermal expansion. Evaporant materials may not be available in the desired rod sizes.

8. The ability to measure the temperature of the molten pool preferably with an optical or total radiation pyrometer. This requires clear visual access to the molten pool and the ability to keep the window free of deposited vapors. The latter devices are commercially available.

D. Temperature Distribution and Thickness Distribution of the Deposit

Consider a flat substrate located at some distance from an evaporation source. For a point source or a small flat plate source the vapor density will decrease proportional to cos θ, where θ is the angle between the vertical axes of the source and the location on the substrate (Cosine distribution law). Thus the deposit will be tapered from the center to the edge. This is not too desriable as it will affect the specimen yield (i.e., the number of specimens that can be machined from a deposit without grinding it to uniform thickness) as well as the temperature distribution from the center to the edge of the specimen. The percent thickness variation from center to edge on a deposit varies with the distance between source and substrate and usually becomes less than 10% at source-substrate distance of 10 times the source diameter. In electron beam heated sources the thickness variation is somewhat greater than that produced by other sources and also depends on the particular material being evaporated. The total thickness per unit time also varies inversely as the square of the source-substrate distance. Therefore, a calculated estimate of the deposit thickness and thickness variation as a function of source-substrate distance is necessary for proper planning of the experiment. One method of producing uniform thickness deposits is to collect them on rotating substrates with the rotation axis inclined about 30° to the horizontal plane. For electron beam sources, the exact angle would have to be determined by experimentation.

The deposition temperature is very important. At very low deposition temperatures the deposit will not be fully dense. At higher deposition temperatures, the deposit will be fully dense. The grain size of the deposit will coarsen as the deposition temperature gets higher. Since the strength and toughness of a deposit decrease with increasing grain size, the selection of the deposition temperature becomes a very important process variable. It should be high enough to produce a fully dense deposit and yet not too high to permit grain size coarsening.

An estimation of the temperature of a deposit produced by high rate physical vapor deposition processes is somewhat complicated. A new method has been developed for making such a calculation by performing an energy balance between energy gain and energy loss of the deposit. The deposit receives energy from three sources -

1. Radiation from the hot source.
2. Latent heat of condensation of the vapor and cooling of the deposit to the deposition temperature.
3. Heat of reaction when a deposit species reacts with the gas phase to form a compound. This is applicable in the case of reactive evaporation only.

In a vacuum environment where the substrate is supported so as to minimize conductive heat transfer to the holder, the principal mode of heat loss is radiative. Radiative heat loss occurs from the deposit face as well as the back side of the substrate. In addition, there is a small energy loss necessary to heat the substrate to the experimental temperature; however this factor is small for these substrates and is zero once equilibrium has been established. The time to attain equilibrium is usually less than a

minute and in most cases a very small fraction of the total deposition time.

The experimental variables are:

1. Nature of evaporating species (metal, alloy, compound) and the vapor pressure of the component species.
2. Temperature of the source and evaporation rate.
3. Source diameter.
4. Source-substrate distance.
5. Substrate material.
6. Substrate material thickness.
7. Thermodynamic properties of condensate (latent heat of condensation, specific heat, vapor pressure).
8. Heat of reaction in the case of reactive evaporation.
9. The total hemispherical emittance of the evaporant as a function of evaporation temperature.
10. The total hemispherical emittance of the deposit as a function of condensation temperature.
11. The total hemispherical emittance of the substrate as a function of condensation temperature.
12. The absorptance of the deposit as a function of condensation temperature.

With a large number of variables, it is essential to make a computational estimate of the temperature distribution of the deposit to minimize the number of experiments performed. A computer program has been written to make such an estimate.

A detailed treatment of these calculations has been reported previously and published in the open literature.[12,13]

E. Synthesis and Characterization of Metal Deposits

The objective of this part of the investigation was to produce Nickel sheets and characterize the structure and mechanical properties. The latter vary as a function of the deposition temperature in accord with the Movchan-Demchishin structural relationship between microstructure and properties.[14] Characterization of the material was carried out by determination of grain size, grain morphology, density, tensile properties bend ductility, and hardness. Samples of wrought (cast, rolled and annealed) nickel foils were also subjected to the same testing procedures in order to form a basis of comparison for the vapor deposition technique.

The deposited nickel foils were produced by high rate physical vapor deposition (HRPVD) techniques. This process was carried out in high vacuum by evaporation of a 2" (nominal) diameter nickel billet placed in a rod-fed electron beam heated source. Figure 1 shows a schematic representation of the deposition set-up. Nickel vapors were condensed on a flat, rotating substrate located above the molten pool. In order to produce a uniform thickness distribution in the deposit, the substrate axis was tilted 30° from horizontal. All substrates were preheated prior to deposition by a spiral tungsten wire, radiant heater located behind the substrate. Temperature was monitored and controlled by use of a chromel-alumel thermocouple spot-welded to the substrate.

The substrate material was .005" thick, 11" diameter stainless steel. Removal of the deposited nickel foil from the substrate was facilitated by application of a thin halide film on the stainless steel prior to evaporation of the nickel.

The wrought nickel foils were cold-rolled from slabs cut from the same billet used in the evaporation process. Samples were 95% cold-worked and then recrystallization annealed in a vacuum of 10^{-5} torr.

For nickel, based on the Movchan-Demchishin model, the boundary temperature between zone 1 and zone 2, T_1, is 245°C (473°F) and between zone 2 and zone 3, T_2 is 504°C (939°F). Table II lists the deposition temperatures, grain sizes and thicknesses of the samples. The morphology of the Ni deposits conformed closely to the nickel deposit morphology reported by Movchan and Demchishin.[14] Figure 3 shows photomicrographs of typical deposited nickel sheet exhibiting zone 2 and zone 3 morphology. In the deposits at 260°C (500°F), 329°C (625°F) and 426°C (800°F) condensation temperatures, typical zone 2 morphology is exhibited. The cross-section shows columnar grains, with the surface structure being equiaxed. In the sample synthesized at a deposition temperature of 554°C (1030°F) the morphology was equiaxed in both directions. This represents a transition from zone 2 to zone 3 morphology. The range of grain sizes in the deposits was from 3.7μ to 26.5μ. In the rolled foils, the grain sizes were controlled by varying the time and temperature of annealing. All samples showed an equiaxed grain structure in the surface view, and a slightly elongated morphology in cross-section, with the elongated direction of rolling. Grain size varied from 11.5μ to 25.3μ.

It has been shown previously for the HRPVD process that if substrate temperature is greater than .25 T_m, the deposit will be fully dense. The present work is consistent with this earlier observation. The density value for both rolled and annealed samples was 8.8 ± 0.1 g/cm^3, The handbook value for nickel is 8.9 g/cm^3.

A. Surface View of Sample Ni-8 Showing Equiaxed Zone 3 Morphology. Deposition Temperature 554°C. (300X)

Cross-Sectional View of Sample Ni-8 Showing Equiaxed Zone 3 Morphology. (200X)

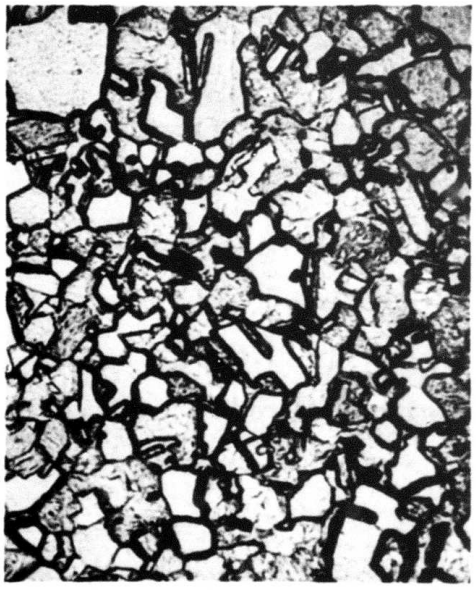

C. Surface View of Sample Ni-9 Showing Equiaxed Zone 2 Morphology. Deposition Temperature 426°C. (300X)

D. Cross-Sectional View of Ni-9 Showing Columnar Zone 2 Morphology. (250X)

Figure 3. Photomicrographs of Typical Nickel Deposits.

In Table I, the yield stress, ultimate tensile strength, percent elongation, and percent reduction in area are shown for the deposited and rolled samples. It is seen that both materials exhibit very similar properties. The Hall-Petch relationship was investigated for yield stress by plotting these values against the inverse square root of the average grain diameter.

The Hall-Petch relationship is:

$$\sigma_y = \sigma_o + K_y d^{-1/2}$$

where σ_y = yield stress

σ_o = Hall-Petch intercept - a measure of the stresses necessary to move dislocations in a grain without resistance from grain boundaries

K_y = the Hall-Petch slope - a measure of grain boundary resistance to slip at yield

The value of the Hall-Petch slope is altered by impurity atoms in the matrix, since this slope is an indication of dislocation locking by solute atoms. For the deposited nickel σ_o = 5.46 Kg/mm^2 and K_y = 1.17 Kg/mm$^{3/2}$. The Hall-Petch constants for the rolled and annealed sheet are σ_o = 2.62 Kg/mm^2 and K_y = 1.64 Kg/mm$^{3/2}$. Possible reasons to explain the difference in the Hall-Petch constants between the as deposited and the rolled and annealed material are: 1) higher impurity content in the rolled foils; and 2) morphology differences in the grain structures as discussed above. Figure 4 shows the Hall-Petch plot for yield stress of nickel versus the inverse root of the average grain diameter. As can be seen, the data is in good agreement with the Hall-Petch relationship.

To determine whether residual stresses were affecting the mechanical properties of the deposited structure, samples of the deposited

Table I

Mechanical Properties of Nickel

Sample	Method of Preparation	Grain Size(μ)	Yield Stress (.2%)(KSI)	Ultimate Tensile Strength (KSI)	% Elongation	% Reduction in Area	$d^{-1/2}$ ($mm^{-1/2}$)	DPH Hardness (Kg/mm^2)
Ni-8	Deposited	26.5	18.4	48.1	39.0	20.8	6.14	96.6
Ni-9	Deposited	19.0	19.2	47.9	32.5	20.7	7.25	109.1
Ni-10	Deposited	12.7	22.6	51.6	34.5	21.4	8.87	103.7
Ni-10*	Deposited and Stress Relieved	12.7	23.0	52.4	26.0	16.3	8.87	-
Ni-12	Deposited	3.7	35.1	57.2	21.6	21.1	16.45	125.1
Ni-12*	Deposited and Stress Relieved	3.7	34.8	56.4	16.0	12.0	16.45	-
Ni-R-1	Rolled and Annealed	20.5	20.4	58.7	50.7	33.2	6.98	93.0
Ni-R-3	Rolled and Annealed	18.0	20.6	57.6	44.5	30.0	7.45	90.8
Ni-R-4	Rolled and Annealed	11.5	25.5	60.9	45.0	27.2	9.33	92.5
Ni-R-5	Rolled and Annealed	25.3	18.3	56.3	54.6	34.2	6.29	89.0

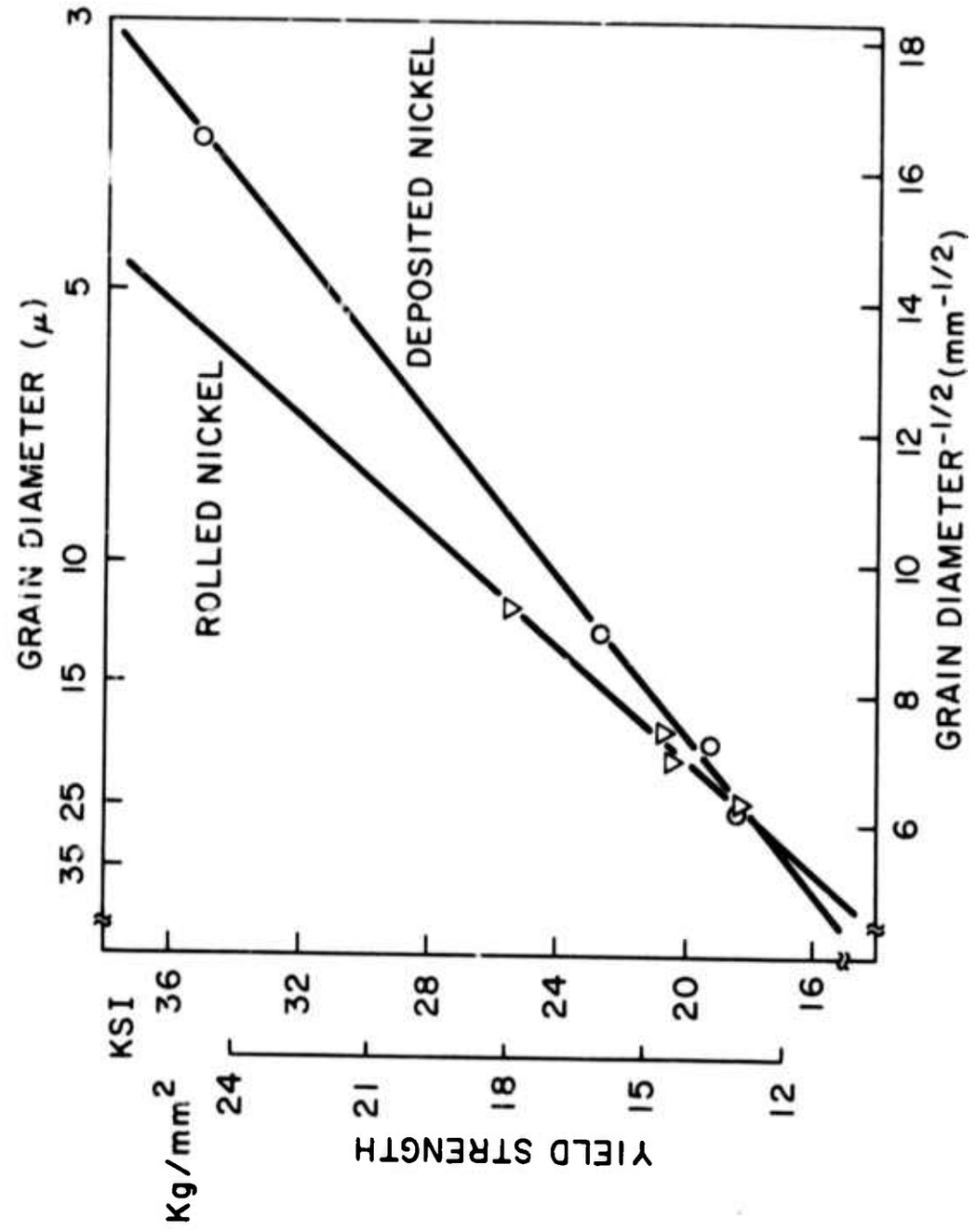

Figure 4. Yield Stress Versus Inverse Square Root of Average Grain Diameter.

material were given a stress-relief treatment for two hours at 300°C. Testing of these showed no change in tensile properties as shown in Table I.

Although the Hall-Petch relationship was developed originally to explain the dependence of yield stress on microstructure, subsequent work by Armstrong[29] and Bunshah and Armstrong[30] has shown that the same type of equation can be used to explain the relationship of hardness to grain size. This Hall-Petch type relationship is:

$$H = H_o + K_H d^{-1/2}$$

where H_o and K_H are experimental constants analogous to the above mentioned Hall-Petch yield stress constants. Table I presents the results of hardness testing. For the deposited nickel $H_o = 85.23$ Kg/mm^2 and $K_H = 2.42$ Kg/mm$^{3/2}$. The rolled and annealed sheet had $H_o = 85.24$ Kg/mm$^{3/2}$ and $K_H = 0.81$ kg/mm$^{3/2}$. The plot of the hardness versus the inverse square root of the average grain diameter is linear. The hardness of the deposited samples is a few percent higher than the rolled and annealed foils. This shift is in agreement with the slightly larger ductility shown in the rolled foils.

The bend ductility of all samples proved to be identical, being able to withstand a < 1T 180° bend at room temperature. Study of the bent edge under magnification showed no sign of cracking or tearing.

In summary, nickel foils of full density were produced by high rate physical vapor deposition techniques. The grain size and grain morphology was varied by changing the substrate temperature. Mechanical tests on the deposited material showed strength and ductility values comparable to similar purity cast, rolled and annealed material. The yield strength and hardness values varied linearly with the inverse square root of the average grain

diameter according to the Hall-Petch relationship. It is therefore concluded that nickel produced by HRPVD techniques is an engineering material.

The complete results have been published in the open literature.[15]

F. Deposition and Characterization of Alloys

Two choices are available for alloy deposition - multiple sources and single sources.

1. Multiple Sources

This is the more versatile system. The number of sources evaporating simultaneously is equal to or less than the number of constituents in the alloy. The material evaporated from each source can be a metal, alloy, or compound. Thus, it is possible to synthesize a dispersion strengthened alloy, e.g. Ni-ThO_2. On the other hand, the process is complex because the evaporation rate from each source has to be monitored and controlled separately. For high deposition rates, this is difficult and tedious. Furthermore, the source to substrate distance would have to be sufficiently large (15 inches for 2 inch dia. sources) to have complete blending of the vapor streams prior to deposition, at least in the center portion of the deposit, which increases the deposition rate. Moreover, with a gross difference in density of two vapors, it may be difficult to obtain a uniform composition across the width of the substrate due to collisional scattering of the lighter vapor atoms.

It is also possible to evaporate each component sequentially thus producing a multi-layer deposit, which is then homogenized by annealing after deposition. This procedure makes it even more difficult to get high

deposition rates. A multiple source arrangement for production of alloy deposits at high rates is not known.

2. Single Source

The disadvantages of multiple sources for alloy deposition can be avoided by using a single source. They can be wire-fed[16] or rod-fed sources,[17] the latter being shown in Fig. 5. There is a molten pool of limited depth above the solid rod. If the components of an alloy, A_1B_1, have different equilibrium vapor pressures, then the steady state composition of the molten pool will differ from the feed rod, e.g. A_1B_{10}. Under steady state conditions, the composition of the vapor is the same as that of the solid being fed into the molten pool. To attain the steady state pool composition, one has the choice of starting with a button of appropriate composition A_1B_{10} on top of a rod A_1B_1 to form the molten pool initially, or one can start with a rod of alloy A_1B_1 and evaporate until the molten pool reaches composition A_1B_{10}. Thus one has a "transient period" during which the pool attains proper composition for the "steady-state" deposition of the alloy. Precautions to be observed are that the temperature and volume of the molten pool have to be constant to obtain a constant vapor composition. A theoretical model has been developed in the course of this program which enables one to calculate the "transient period" as a function of the properties of the constituents of the alloy, the size of the evaporant rod, and the temperature of the molten pool. This model has been confirmed experimentally for the evaporation and deposition of a Ni-20Cr alloy. The complete details of this part of the investigation have been reported previously and published in the open literature.[17] In addition to Ni-20Cr deposits, other alloys deposits such as Ti-6Al-4V, Ag-5Cu, Ag-10Cu, Ag-20Cu, Ag-30Cu, M-xCr-yAl-zY alloy (where M can be Ni, Fe, or Co)

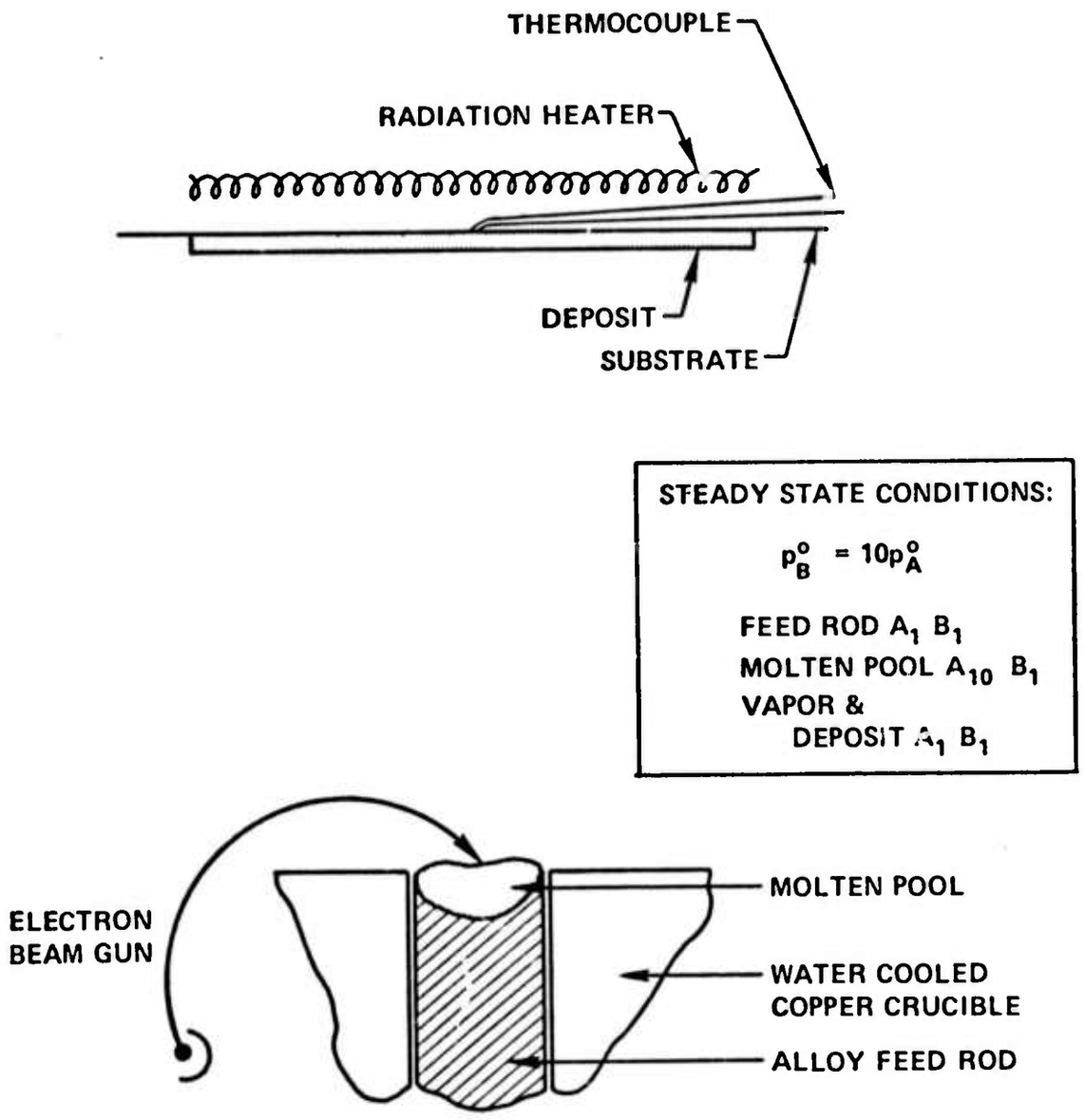

Figure 5. Schematic of Direct Evaporation of an Alloy from a Single Rod-Fed Source.

deposits have been successfully prepared. To date, experimental results indicate that this method can be used with vapor pressure differences of a factor of 5000 between the components. This method cannot be used where one of the alloy constituents is a compound, e.g. Ni-ThO_2.

Similar to the work in Ni above, Ni-20Cr alloy sheet was prepared by HRPVD techniques. The structure of the deposit was varied as a function of the deposition temperature and the mechanical properties were evaluated at ambient and elevated temperatures. The complete results are to be published in the open literature[18] and are included in this report as Appendix I.

G. Synthesis, Deposition and Characterization of Compounds

The process of Direct Evaporation (i.e. evaporant and deposit being the same material) for the deposition of oxides[14] and other compounds[19] has been reported. However, in our experience, this presents two problems. One, partial dissociation of the compound can occur, resulting in a deposit of a different composition from the source. Thus, direct evaporation of Al_2O_3 results in an oxygen deficient film[21] which can only be restored to stoichiometry by evaporation in the presence of a partial pressure of oxygen or possibly a post-deposition anneal in oxygen. Two, for high melting point compounds such as Al_2O_3, TiC, etc., a high power density source has to be used to obtain appreciable evaporation rates which result in a physical disintegration of many compound evaporant billets (prepared by pressing and sintering of powders).

Therefore, we prefer to use the Reactive Evaporation (RE) [22] or the Activated Reactive Evaporation (ARE) processes[23] for the deposition of compounds. In these processes, metal or alloy vapors are produced in the

presence of a partial pressure of reactive gas to form a compound either in the gas phase or on the substrate as a result of a reaction between the metal vapor and the gas atom (Reactive Evaporation) e.g.

$$2Y + \frac{3}{2} O_2 \rightarrow Y_2O_3$$

or

$$Ti + \frac{1}{2} C_2H_2 \rightarrow TiC + \frac{1}{2} H_2$$

The reaction may be encouraged to go to completion by activation and/or ionizing both the metal and gas atoms in the vapor phase as shown in Fig. 6, in which case it is called the ACTIVATED REACTIVE EVAPORATION PROCESS. This is a NEW PROCESS which was developed during this investigation for the high rate deposition of high melting compounds, such as oxides, carbides, nitrides, etc.; and has been granted a U.S. Patent.[23] In this process, the molten metal, heated by a high acceleration voltage electron beam, has a plasma sheath on top of the pool from which the low energy secondary electrons are pulled upwards into the reaction zone by an electrode placed above the pool biased to a small positive potential (20 to 100V). These low energy electrons have a high ionization cross-section thus ionizing or activating the metal and gas atoms and increasing the reaction probability on collision. The synthesis of TiC by reaction of Ti metal vapor and C_2H_2 gas atoms with a carbon/metal ratio approaching unity was achieved with this process.[24] Moreover, by varying the partial pressure of either of reactants the carbon/metal ratio of TiC, ZrC and (Hf-Zr)C could be controlled to produce any desired value,[25] as shown in Table II. Without activation, i.e. Reactive Evaporation, there was no control on the composition of the deposit which could be just Ti or Ti + TiC on all TiC of variable C/Ti ratio.

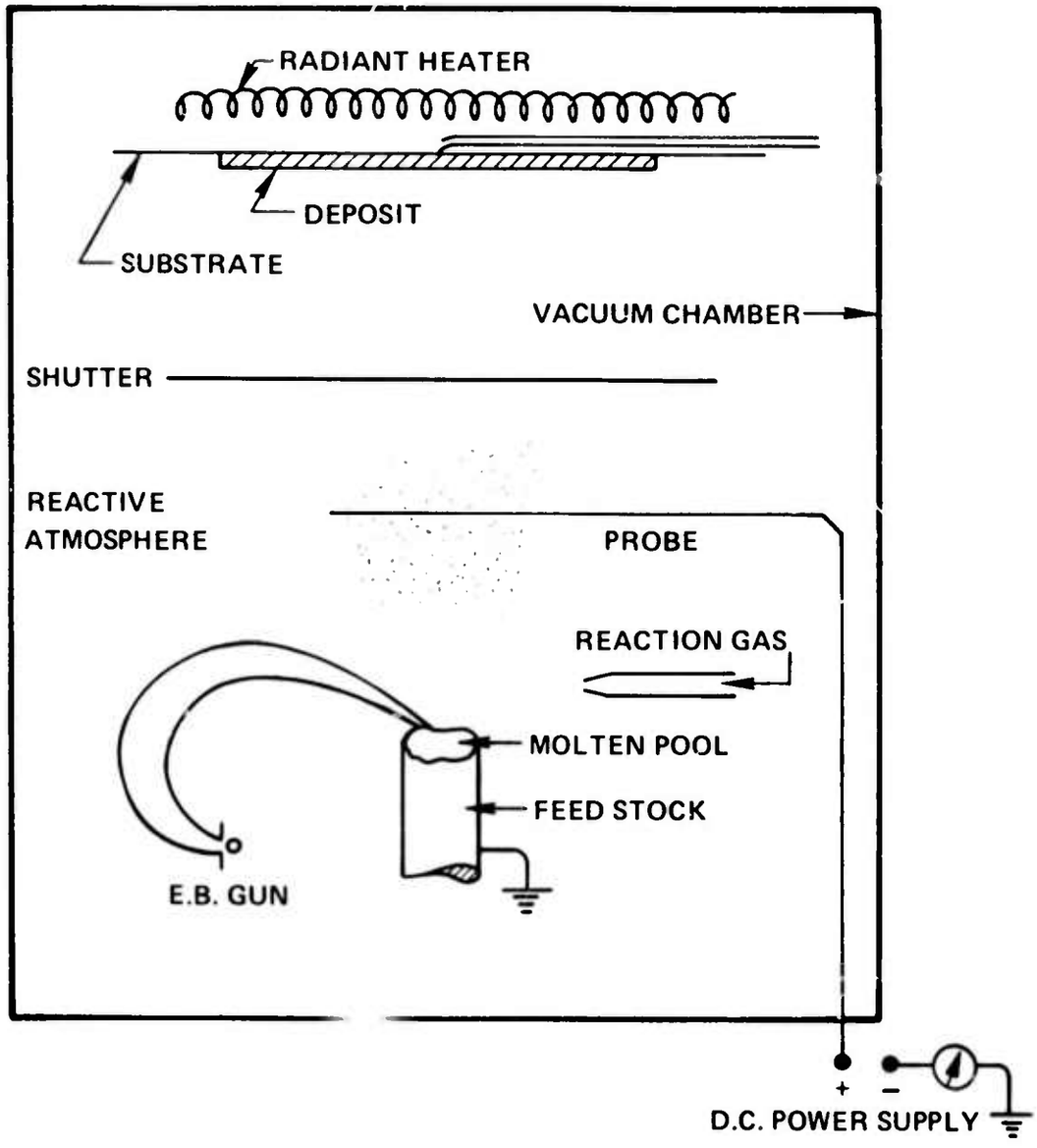

Figure 6. Schematic of the Experimental Arrangement for the Activated Reactive Evaporation Process.

Table II

Variation of Lattice Parameter, $[\frac{C}{M}]$ Ratio and Microhardness with Pressure of Reactive Gas for TiC

Sample	$P_{C_2H_2}$ torr	Rate of Evaporation g/min	Rate of Deposition m/min	Lattice Parameter Å	Combined Carbon to Metal Ratio $[\frac{C}{M}]$	Microhardness (50 g load) DPHN kg/mm^2	Particle Size <D> in A	Strain ε_{111} in %
	1×10^{-4}	0.67	4	-	Ti + TiC	-		
34-4	3×10^{-4}	0.67	4	4.308±.003	0.5-0.6	2,000	180	0.33
35-3	4×10^{-4}	0.67	4	4.317±.002	0.62-0.64	2,550	160	0.74
	5×10^{-4}	0.67	4	4.322±.003	0.64-0.70	2,775	-	-
34-6	$7-8 \times 10^{-4}$	0.67	4	4.329±.001	0.73-0.96	2,670	200	0.21

Variations of the reactive evaporation process proposed in the literature have activated the gas outside the reaction zone using glow discharge or microwave discharge.[26] This procedure would not be adequate for high rate compound deposition since activated gases become deactivated on collision with other gas molecules or on surfaces in the gas path, e.g., those of the tube through which the gas flows. In the ARE process, the activation of both the metal and gas reactants is produced constantly in the REACTION ZONE between the source and the substrate which is what is needed for the high rate deposition of compounds.

Table III gives an example of the various compounds that were synthesized in this ivnestigation.

As stated earlier, the deposition temperature is a very important process variable which strongly influences structures and properties. Deposits of Y_2O_3 and TiC of a fixed anion/cation ratios were prepared at various substrate temperatures. The microstructures exhibited the zone 1 and zone 2 morphologies of the Movchan-Demchishin model.[14] Surface and fracture cross-sections of TiC deposits synthesized at temperatures from 500 to 1450°C are shown in Fig. 7. In this figure it is shown also that the zone 1 to zone 2 transition in morphology can also be obtained by depositing 560°C (zone 1) and heat treating to 1180°C for 1 hour to obtain the zone 2 morphology. Microhardness measurements on Y_2O_3 and TiC deposits as a function of the deposition temperature are given in Figs. 8 and 9 respectively. Figure 10 shows a similar plot from Movchan-Demchishin's data[14] for Al_2O_3 and ZrO_2. As shown in Fig. 9, by changing the deposition temperature of TiC from 500°C to 1080°C, a very marked change occurs in the hardness of the deposit from 3000 to 5500 kg/mm^2. The latter is a hardness value second

TABLE III

Experimental Conditions for the Reactive and Activated Reactive Evaporation of Compounds

Evaporant and Reactive Gas	Reactive Atmosphere		$T_{substrate}$ °C	Rate of deposition μm/min	Species Obtained
	P_{gas} torr	w or w/o potential on probe			
1. Y-O_2-2	1.10^{-4}	w/o or with potential	Room temp.	13.0	Y_2O_3
2. Ti-$N_2$9	4.10^{-4}	"	"	4.0	Ti+TiN
3. Ti-N_2-8	4.10^{-4}	w/potential	"	3.0	TiN
4. Ti-NH_3-2	4.10^{-4}	"	"	3.0	TiN
5. Ti-C_2H_2-34	5.10^{-4}	"	450	4.0	TiC
6. Zr-C_2H_2-1	4.10^{-4}	"	540	5.0	ZrC
7. Hf-C_2H_2-2	4.10^{-4}	"	515	2.5	(Hf-3Zr)C
8. V-C_2H_2-5	5.10^{-4}	"	555	3.0	VC
9. Nb-C_2H_2-2	4.10^{-4}	"	540	2.5	NbC
10. Ta-C_2H_2-2	4.10^{-4}	"	590	1.5	TaC

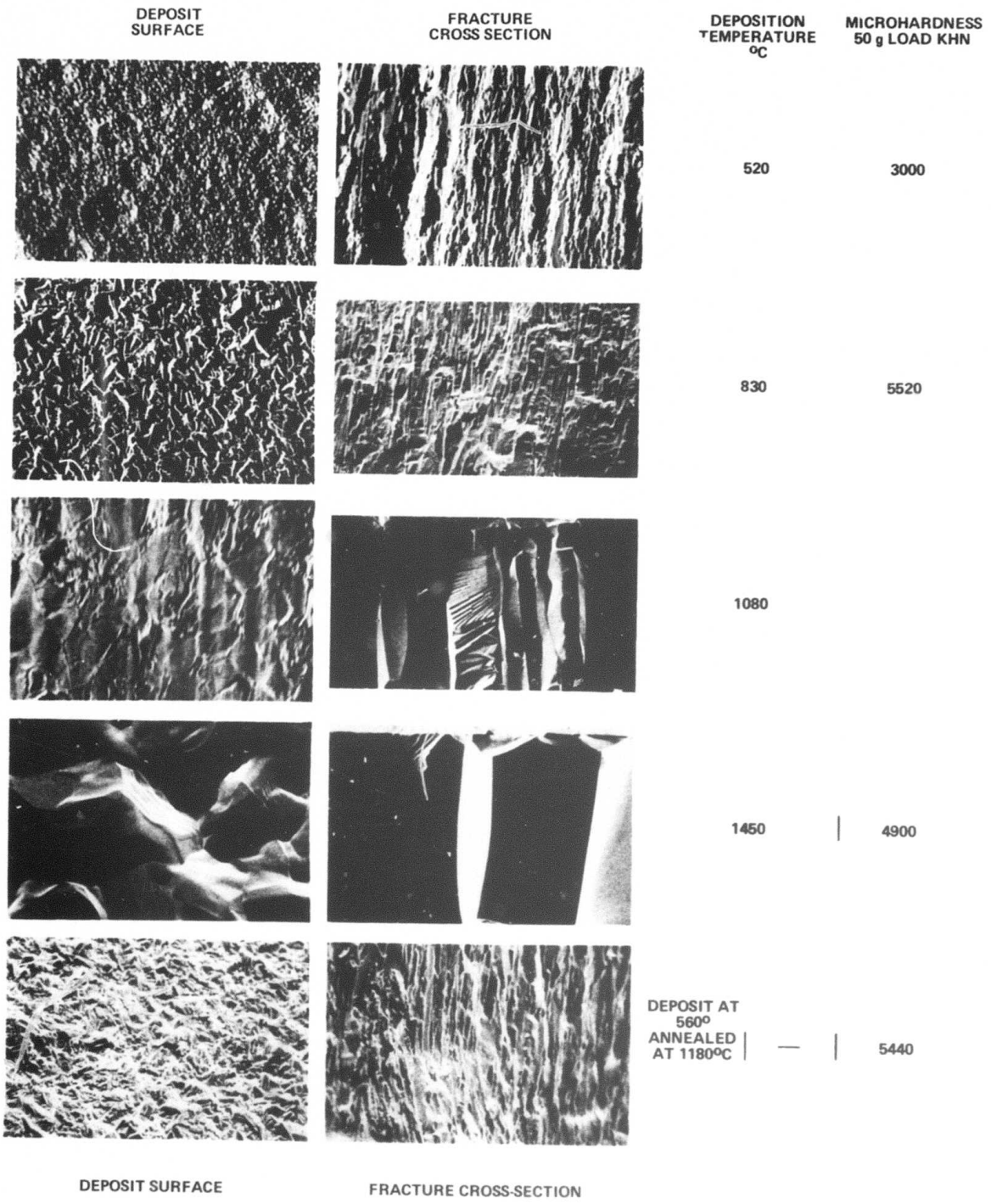

Figure 7. Structure and Microhardness of TiC Deposits at Various Substrate Temperatures (Raghuram and Bunshah). (1000X).

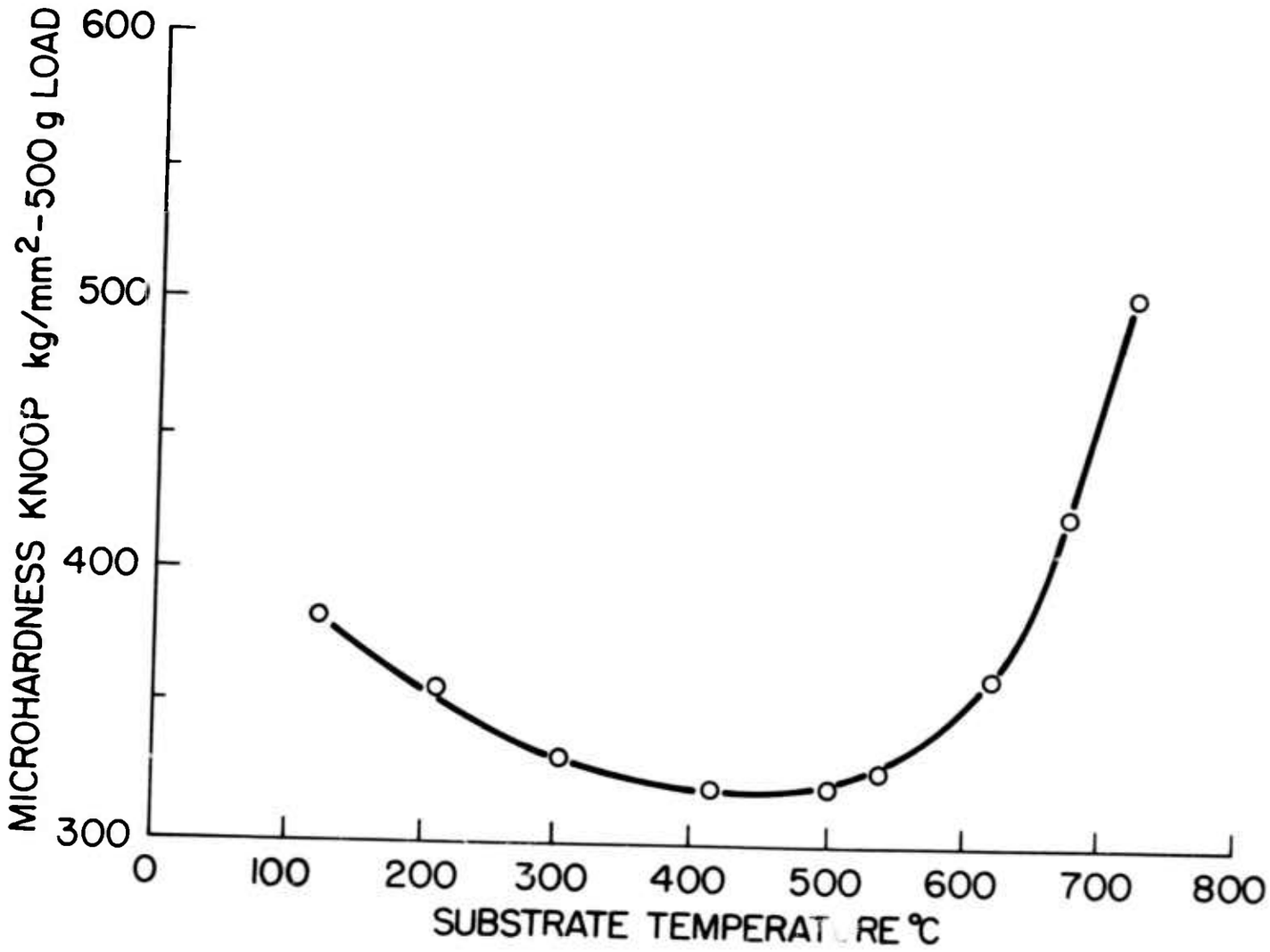

Figure 8. Microhardness vs Deposition Temperature for Y_2O_3 Deposits.

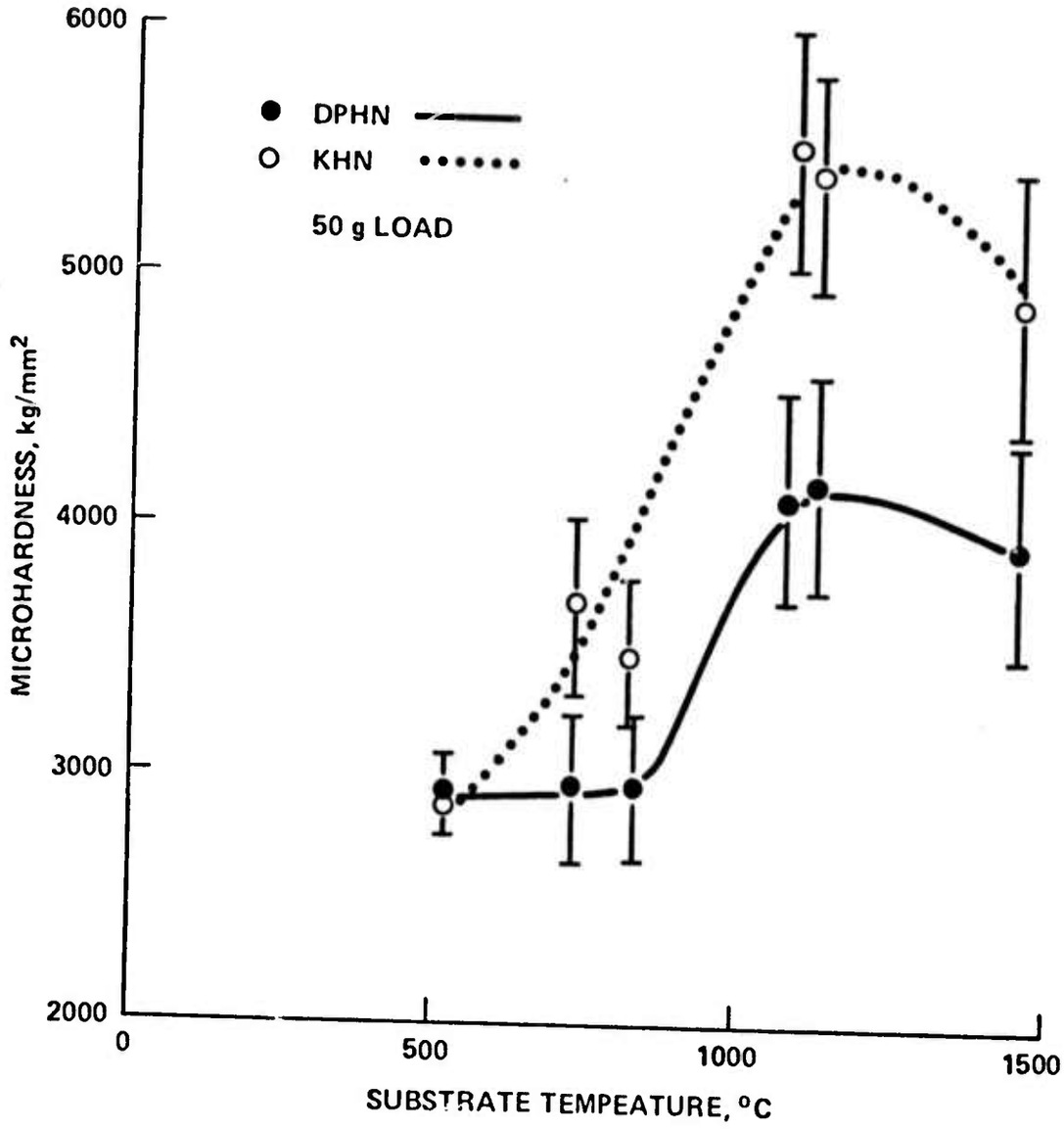

Figure 9. Microhardness vs. Substrate Temperature for TiC Deposits at Constant C/M Ratio.

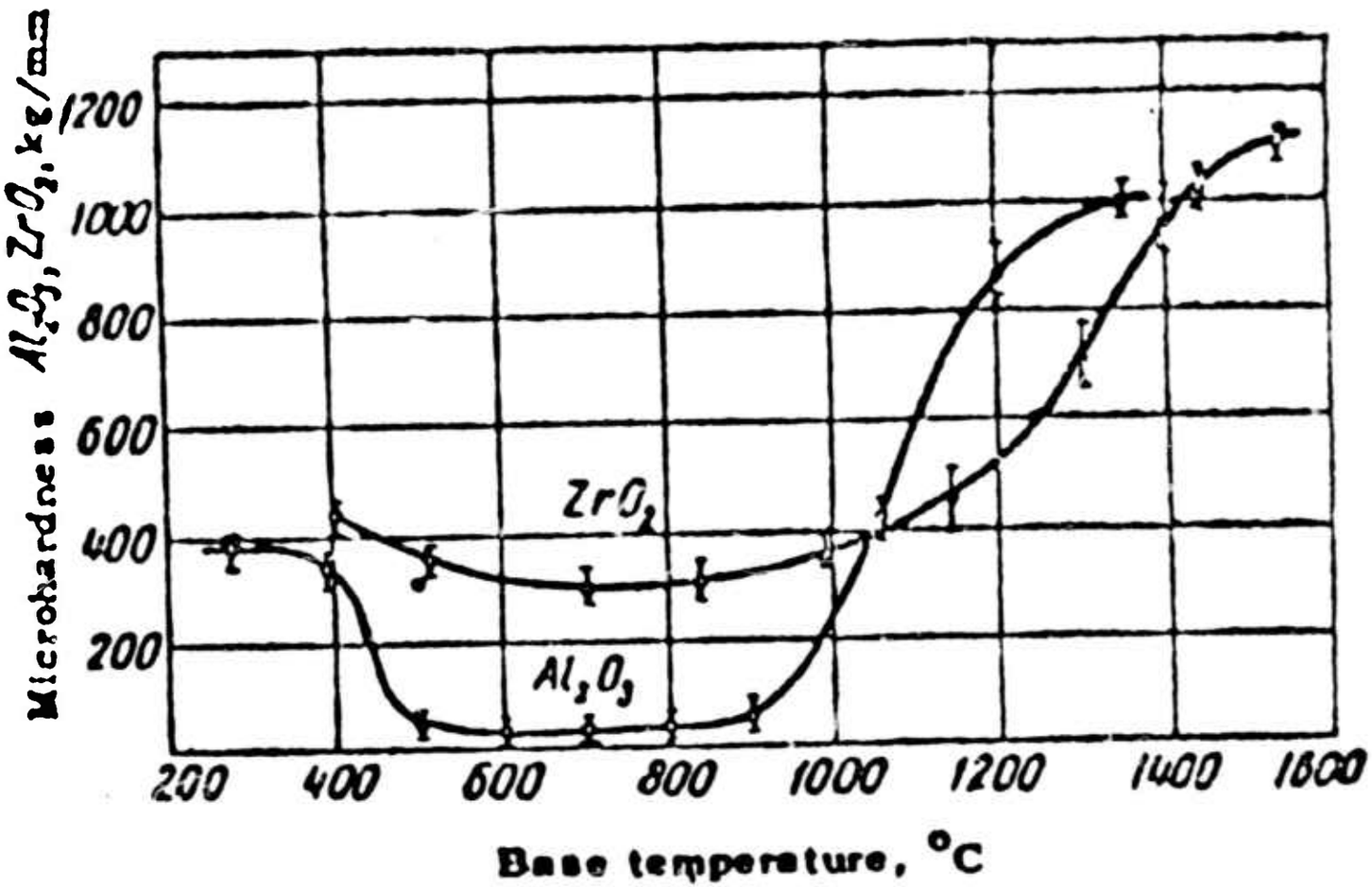

Figure 10. Microhardness vs. Deposition Temperature for Al_2O_3 and ZrO_2. (Movchan and Demchishin)

only to that of diamond as shown in Table IV. A simple explanation for this increase in hardness of compound deposits with higher deposition temperatures is the observation that the microstructure contains fewer flaws Since compounds are extremely sensitive to the presence of flaws, this decrease in flaw content is reflected by a marked change in hardness as observed for Al_2O_3, ZrO_2, Y_2O_3 and TiC. Further evidence of this is derived from x-ray diffraction studies. The high temperature deposits show very sharp diffraction peaks thus indicating a much lower level of residual stress than low temperature deposits where the peaks are broad.

H. Deposition and Characterization of Dispersion Strengthened Alloys

This part of the investigation is concerned with the feasibility of producing deposits of dispersion strengthened alloys by HRPVD techniques. One method to achieve this objective is to evaporate the matrix metal or alloy from one source, and the dispersed phase from a second source. Paton[20] and coworkers have demonstrated the deposition of Ni-TiC and Ni-ZrO_2 alloys using two-source deposition. They were able to obtain very fine dispersed phase particles (100-1000Å) and correspondingly small interparticle spacing, 100-1000Å. In fact, high temperature tests on the Ni-ZrO_2 alloy at 1300°C showed that the alloy had good high temperature strength and the dispersion was stable, i.e., did not agglomerate.

In this investigation, we explored the synthesis of a dispersion strengthened alloy by evaporation of an alloy billet from a single rod-fed source and reacting one of the components with a reactive gas to form a compound using the ARE process. A Ni-Ti alloy was evaporated in the presence of a partial presence of C_2H_2 to form a Ni-TiC alloy. This could be accomplished since the Ti reacts to form TiC and the Ni does not form a carbide.

TABLE IV

Hardness of Various Compounds

Material	Hardness (Kg/mm^2)
Diamond	7,000
TiC (UCLA, High deposition temperature 1000°C)	5,500
Borazon (cubic boron nitride)	4,500
Rare-earth borides	3,500--4,000
TiC (commerical and UCLA low deposition temperature -500°C)	3,000
Silicon carbide	2,500
Aluminium oxide	2,100
Tungsten carbide	1,700
Quartz	820
Metals	< 800

The microstructure of the deposit shows a fine dispersion of TiC in a Ni matrix and the hardness is increased from 138 to 1000 kg/mm^2. This work has been presented at the Second Conference on Structure/Property Relationships in Thick Films and Bulk Deposits and submitted for publication.[31] The details of the study are included as Appendix II to this report.

I. Gas Scattering Evaporation

One of the characteristics of the evaporation process is the observation that deposition occurs on a substrate located in the line-of-sight of the source. Substrate surfaces which do not "see" the deposit are not coated. This limitation occurs because of the very large mean free path of the vapor atoms so that they travel in a straight line from source to substrate without collisions. However, if one introduces a gas in the vacuum chamber whose partial pressure is in the micron range, the mean free path becomes much smaller, of the order of a few mm. Then, the vapor atoms suffer multiple collisions in their travel from the source to substrate and a substrate can be coated on all sides.

The effect of the presence of a gas during physical vapor deposition experiments using an electron beam heated source was studied. Some of the parameters studied are reactive vs. non-reactive gases including varying the process to include activated reactive evaporation; gas pressure; condensation rate vs. evaporation; the efficiency of plating on the back side of the substrate, i.e., non-line-of-sight from the evaporant source; and deviations from the cosine law distribution vs. gas type and pressure. The results show greater plating efficiencies with reactive gases than non-reactive gases at similar pressures. As expected, when the

pressure is increased to high values (> 50μ), the process efficiencies decrease. The efficiency for non-line-of-sight plating was found to depend primarily upon the atomic mass of the gas and secondarily upon the gas pressure.

The resultant microstructure is not fully dense and shows lower hardness than those of coatings produced in direct line of sight. This problem can be remedied by increasing the surface mobility of the depositing species by increasing the substrate temperature or the kinetic energy of the vapor atoms. The results have been reported previously in a Progress Report and in the open literature.[27]

III. THE PROPERTIES OF RARE EARTH METALS AND ALLOYS

In this part of the investigation, the thrust was directed towards elucidating the Oxidation Mechanism of Ni_3Al containing yttrium.

The high-temperature oxidation behavior of Ni_3Al (Ni-13.2 wt.% Al) with and without additions of 0.5 wt.% Y has been studied over the range of 900-1200°C in air. None of the commonly accepted rate laws were followed by the kinetics. Although the weight gains of samples containing Y were consistently 10-20% greater than those without Y, the steady-state scaling rates were identical. A quantitative X-ray diffraction technique was used to determine the kinetics of growth of the protective alpha-alumina layer (one of several oxides formed). The alumina growth followed the parabolic rate law under all conditions studied. The rate-controlling transport process in alumina was the enhanced diffusion of oxygen down grain boundaries. The presence of Y as Ni-rich intermetallic promoted the formation of Ni aluminate (spinel). A marked increase in scale adherence was observed for short times. At longer times, however, the

outer layer of spinel and unreacted NiO spalled off along with some of the inner alumina layer. Loss of adherence was caused by a complex Y-Al oxide which formed by the solid state reaction of yttria and alumina. The poor scale adherence on Ni_3Al was due to the formation of voids at the alloy-oxide interface. These voids concentrated the athermal stresses above the oxide-to-metal adherence strength. The voids were produced as a result of the selective oxidation of Al resulting from a "Kirkendall" effect in the substrate. During the selective oxidation process, a vacancy flux directed from the matrix to the metal-oxide interface resulted in a supersaturation of vacancies. Equilibrium was maintained by the condensation of excess vacancies. The presence of Y as either Ni-rich intermetallics or internal oxide prevented the voids from forming. The Y-rich particles relieved the matrix of vacancy supersaturation by providing vacancy sinks. The chemical nature of the particles does not seem important. A necessary and sufficient condition for an effective vacancy sink appears to be the presence of an incoherent boundary between particle and matrix.

The detailed studies have been published in the open literature[27] and in a prior Semi-Annual Progress Report.

IV. SUMMARY AND CONCLUSIONS

In the course of this investigation, the high rate evaporation technique has been systematically studied for the deposition of metals, solid-solution alloys, compounds and dispersion strengthened alloys. An important new process, Activated Reactive Evaporation (ARE) has been developed for the high-rate deposition of compounds. It has the unique feature of being able to control the composition, i.e., the cation/anion ratio of the compound deposits.

Another important result of this study has been the influence of deposition temperature on microstructure and morphology of the deposits. It was found that the morphology varied systematically according to the Movchan-Demchishin model for all the single phase materials studied, i.e., Ni, Ni-20Cr, Y_2O_3, TiC. A remarkable result was the observation that the hardness of the compound deposits, Y_2O_3 and TiC increased, and the level of residual stress decreased with deposition temperature. On the other hand, the hardness of metal and alloy deposits decreased with deposition temperature. These results are in agreement with those of Professor Movchan and coworkers in the USSR who also found the increase in hardness with deposition temperature for the compounds Al_2O_3 and ZrO_2 and a decrease in hardness with deposition temperature for the metals, Ni, Ti and W.

The yield strength and hardness of Ni and Ni-20Cr deposits varied linearly with the inverse square root of the grain diameter, thus following the Hall-Petch relationship. The tensile properties and hardness of Ni and Ni-20Cr deposits were very similar to those of the corresponding wrought materials. Thus the full density deposits produced by HRPVD techniques are true engineering materials.

From this investigation, it may be concluded that the ground work has been laid for applying these techniques to such diverse applications as the production of sheet and foil, of hard coatings for wear resistance in engineering and machining applications, of corrosion resistance coatings, of ultrafine powders, etc. The future appears very promising for these techniques to meet the challenge of demanding applications where the material must possess a combination of diverse properties.

In the second part of this study, the oxidation mechanism of Ni_3Al containing yttrium was developed.

Appendix III lists the papers published as a result of the work done on this contract.

References

1. R.F. Bunshah, "Superpurification of Metals by Vacuum Distillation: A Theoretical Study," Trans. Vac. Met. Conf., 1963, AVS, 121.

2. R.F. Bunshah and R.S Juntz, "Purification of Beryllium by Crucible Free Melting and Distillation Process" in Beryllium Technology, Gordon and Breach, 1964, 1.

3. R.F. Bunshah, "Impurity Removal by Distillation of Beryllium from the Solid State," Proceedings, Int'l. Conf. on Beryllium, Grenoble, France, 1965, Presses Universitaries de France, 108 Blvd. St. Germain, Paris, 6, 63.

4. R.F. Bunshah and R.S. Juntz, "The Purification of Beryllium by Vacuum Melting followed by Vacuum Distillation in an Electron Beam Furnace with Simultaneous deposition of Sheet," Trans. Vac. Met. Conf. 1966, AVS, 209.

5. R.F. Bunshah, "The Effect of Purification on Some Mechanical Properties of Beryllium," Metals Engineering Quarterly, Nov. 1964, 8.

6. R.F. Bunshah and R.S. Juntz, "Electron Beam Distillation Furnace for Reactive Metals: Design Considerations and Operating Experience," Trans. Vac. Met. Conf., 1965, AVS, 200.

7. R.F. Bunshah and R.S. Juntz, "Design Considerations for the Production of Massive Deposits of Alloys by Evaporation from Multiple Electron Beam Heated Sources," Trans. Vac. Met. Conf., 1967, AVS, 799.

8. R.F. Bunshah and R.S. Juntz, "Influence of Condensation Temperature on Microstructure and Mechanical Properties of Titanium Sheet," to be published.

9. R.F. Bunshah and R.S. Juntz, Trans. Vac. Met. Conf., 1965, published by American Vacuum Society, p. 200.

10. H.R. Smith Jr. and C.D'A. Hunt, Trans. Vac. Met. Conf., 1964, American Vacuum Society, p. 227.

11. J.F. Butler, J. Vac. Sci. Tech., 7 (1970), p. S52.

12. R. Chow and R.F. Bunshah, J. Vac. Sci. Techl, 8, VM 73 (1971).

13. R. Nimmagadda and R.F. Bunshah, J. Vac. Sci. Tech., 8 VM 85 (1971).

14. B.A. Movchan and A.V. Demchishin, Fiz. Metall. Metalloved., 28, No. 4 (1969) p. 653.

15. N. Kane and R.F. Bunshah, Proc. 4th Int'l. Vac. Met. Conf., Tokyo, Japan, June 1973, published by the Iron and Steel Institute of Japan, p. 242.

Preceding page blank

16. T. Santala and M. Adams Jr., Vac. Sci. Tech. 7 (1970) p. S22.

17. R. Nimmagadda, A.C. Raghuram, and R.F. Bunshah, J. Vac. Sci. Tech., 9 (1972) p. 1406.

18. N. Agarwal, N.F. Kane and R.F. Bunshah, to be published J. Vac. Sci. Tech. 12 (1975).

19. L. Holland, Vacuum Deposition of Thin Films, Chapman and Hall, London (1966).

20. B.A. Paton, B.A. Movchan and A.V. Demchishin, Proc. 4th Int'l. Conf. on Vac. Met., Tokyo, Japan, June 1973, publisher Iron and Steel Institute of Japan, p. 251.

21. D. Hoffman and D. Liebowitz, J. Vac. Sci. Tech. 9 (1972) p. 326.

22. (a) S. Brismaid, et al., U.S. Patent No. 2,784,115 (1957).
(b) M. Auwarter, U.S. Patent No. 2,920,002 (1960).

23. (a) R.F. Bunshah, U.S. Patent No. 3,791,852.
(b) R.F. Bunshah and A.C. Raghuram, J. Vac. Sci. Tech. 9 (1972) p. 1385.

24. A.C. Raghuram and R.F. Bunshah, J. Vac. Sci. Tech. 9 (1972) p. 1389.

25. R. Nimmagadda, A.C. Raghuram, R.F. Bunshah and C.N.J. Wagner, Thin Solid Films, 20, 187 (1974).

26. B.B. Kosicki and D. Khang, J. Vac. Sci. Tech. 6, 592 (1969).

27. H.A. Beale, F. Weiler and R.F. Bunshah, Proc. 4th Int'l. Conf. on Vac. Met., June 1973, published by the Iron and Steel Institute of Japan, p. 238.

28. J.D. Kuenzly and D.L. Douglass, Oxidation of Metals 8, 139 (1974).

29. R.E. Armstrong, I. Codd, R. M. Douthwaite, and N. J. Petch, Phil. Mag. 7, 45 (1962).

30. R.F. Bunshah and R. W. Armstrong, Mat. Res. Bull. 4, 239 (1969).

31. R. Nimmagadda and R. F. Bunshah, "Synthesis of Dispersion Strengthened Alloy by Activated Reactive Evaporation", submitted to J. Vac. Sci. Tech.

APPENDIX I

Structure-Property Relationships in Ni-20Cr Produced by High Rate Physical Vapor Deposition

by

N. Agarwal, N. Kane and R.F. Bunshah
Materials Department
6532 Boelter Hall
University of California at Los Angeles
Los Angeles, California 90024

ABSTRACT

In high rate physical vapor deposition (HRPVD) processes, a change in substrate temperature produces a marked change in microstructure, mechanical properties and hardness of the deposits. By varying this parameter, the relationship between microstructure and mechanical properties of vapor deposited Ni-20Cr sheets was investigated. These sheets were characterized by grain size, grain morphology, density, tensile properties, bend ductility and hardness. The grain morphology of deposited sheets at different substrate temperatures was in agreement with the morphology zone model suggested by Movchan and Demchishin.[1] Samples of wrought (cast, rolled and annealed) sheets from the same material were characterized by the same procedures to form a basis of comparison for deposited sheets. The investigation of mechanical properties and Hall-Petch relationship showed that deposited material was very similar to rolled and annealed material and constitutes a true engineering material.

I. Introduction

The technique for the deposition of full density Ni-20Cr sheet by high rate physical vapor deposition (HRPVD) process has been previously described. The aim of this study is to investigate the relationship between deposition temperature, microstructure and mechanical properties of Ni-20Cr sheet. Characterization of the material was carried out by determination of grain size, grain morphology, density, tensile properties at room temperature and 1000°C, bend ductility and hardness. Samples of wrought (vacuum melted, rolled and annealed) Ni-20Cr sheets from the same lot used for evaporation were also subjected to the identical characterization and testing procedures in order to form a basis of comparison for the vapor deposited material.

II. Experimental Techniques

A. Production of Vapor Deposited Specimens

High rate physical vapor deposition (HRPVD) technique was used to produce Ni-20Cr deposits in the form of sheet. This process was carried out in high vacuum by evaporation of a 2" diameter vacuum melted Ni-20Cr rod placed in a rod-fed electron beam heated source. The process of alloy deposition from a single rod-fed source has been discussed previously by Nimmagadda, Raghuram and Bunshah.[1] Figure 1 shows a schematic representation of the deposition set up. The vapors were condensed on a flat, rotating substrate located above the molten pool. In order to produce a relatively uniform thickness distribution ($\pm$ 10%) in the deposit, the substrate axis was tilted 30° from the horizontal. All substrates were preheated to various pre-selected temperatures by a tungsten wire radiant heater located behind the substrate. Temperature was monitored by a chromel-alumel thermocouple spot-welded to the substrate.

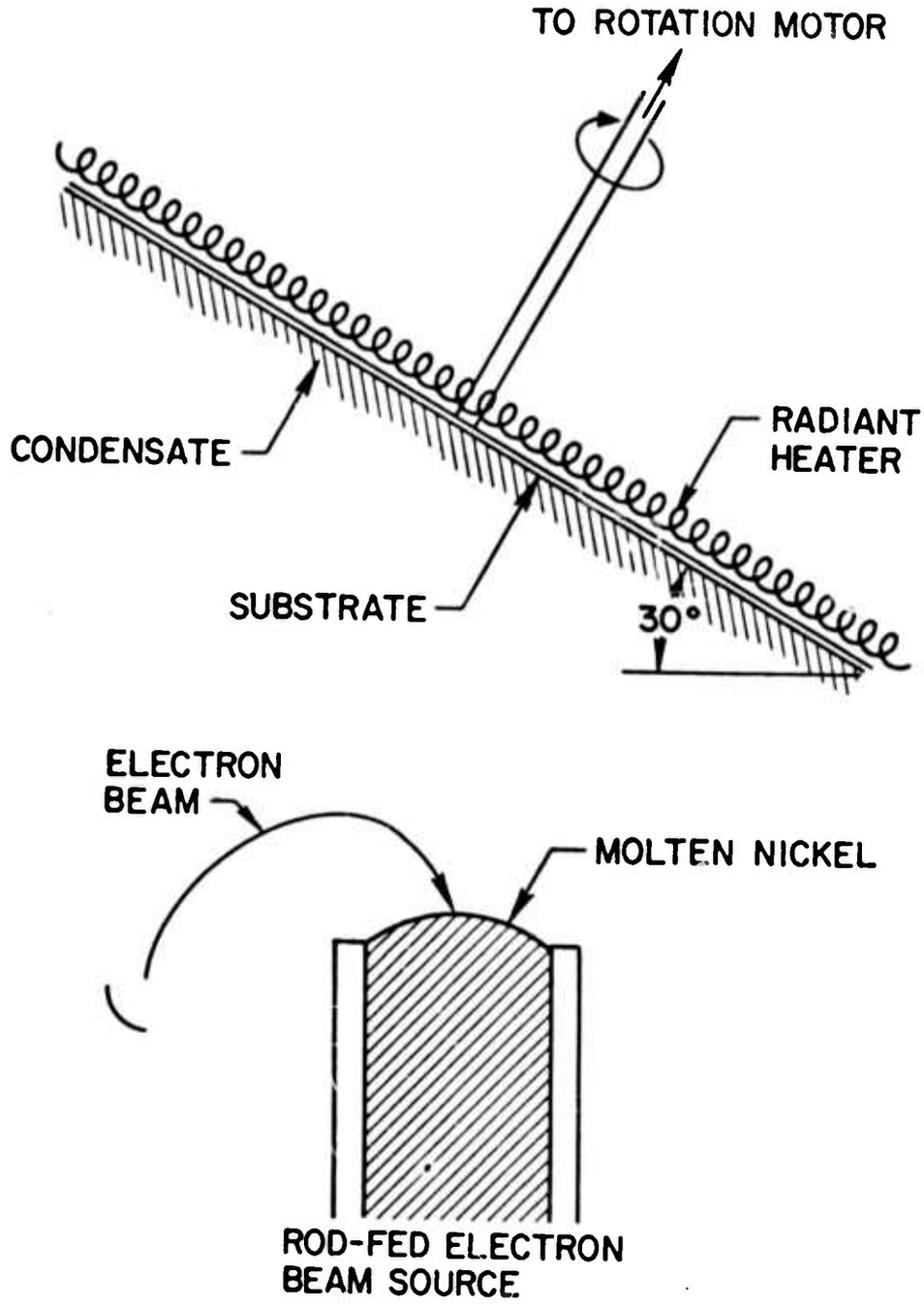

Figure 1. Schematic of Deposition Set-Up.

The substrate material was 0.005" thick. 11" diameter stainless steel sheet. Removal of the deposited Ni-20Cr foil from the substrate was facilitated by application of a thin halide film onto the stainless steel substrate.

B. Rolled Samples

The wrought Ni-20Cr sheets were cold-rolled from slabs cut from the same vacuum melted billet used in the evaporation process. Samples were 95% cold worked and then recrystallization annealed in a vacuum of 10^{-5} torr.

C. Grain Size Determination

The grain size of the deposit was controlled by varying the substrate temperature. In the rolled foil, grain size was controlled by a choice of annealing temperature and time. Standard metallographic techniques were used to mount, polish and etch these specimens. The average grain diameter was determined using a linear intercept method.

D. Mechanical Properties

1. Tensile Properties

Tensile tests were carried out on an Instron machine using a cross-head separation rate of 0.02"/minute to determine their tensile properties 0.2% offset yield stress, ultimate tensile strength, percent elongation and percent reduction in area. The tests were carried out at room temperature (25°C) and at an elevated temperature (1000°C). Tensile specimens were made according to ASTM specification E8-69 for subsize specimens. The deposited samples were tested in both the as deposited state and after a recovery anneal, while the rolled samples were tested after a recrystallization anneal. Multiple samples were used for each data point presented.

2. Hardness

Hardness measurements were carried out on a Tukon Microhardness Tester with a 136° diamond pryamid indentor. Loads used ranged from 100 gm to 600 gm, and a number of measurements were made at each load. The foil samples were mounted in lucite to assure rigidity. The size of indentation was chosen such that multigranular hardness, rather than single grain hardness was being measured.

3. Bend Dubtility

Room temperature bend ductility tests, conforming to ASTM specification E290-88, were performed using wire mandrels of diameter approximating the sample thickness. Samples underwent 180° bends around these mandrels and the bent surface was then checked in a metallograph for any evidence of cracking.

III. Results and Discussion

A. Grain Size and Morphology

In vapor deposited foils the grain size is strongly dependent on the deposition temperature. It has been shown by Movchan and Demchishin[2] that for nickel, titanium and tungsten, three characteristic morphology zones exist in vapor deposited foils. As shown in Fig. 2, these are: Zone 1 - domed surface structure with tapering grains through the cross-section; Zone 2 - columnar grains through the cross section with a smooth surface; and Zone 3 - equiaxed grains in the cross-section surface of the deposit. This model has been confirmed by other work on several metals and compounds.[1,3-6] The change in morphology between Zone 1 and 2 occurs at approximately 0.3 Tm and between Zone 2 and 3 at approximately 0.45 Tm to 0.5 Tm, where Tm is the melting point in °K. These transitions

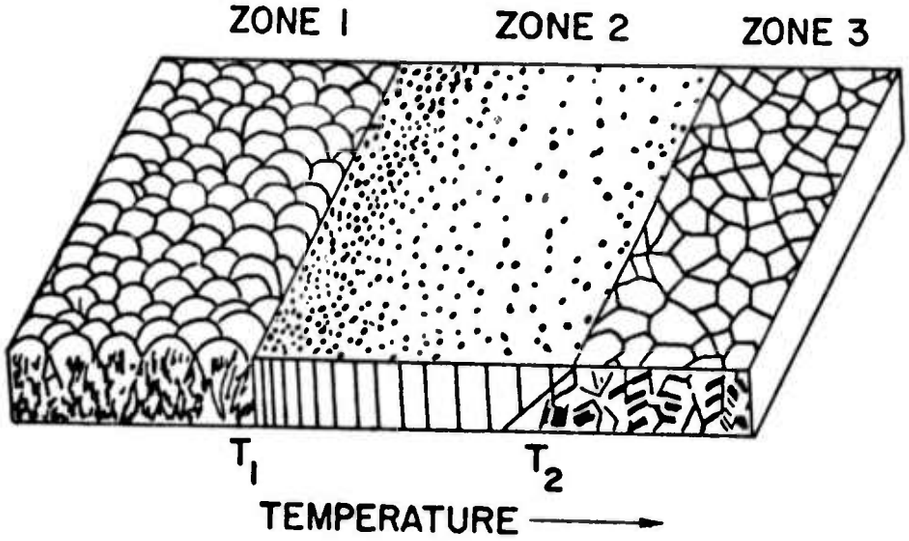

	ZONE 1	ZONE 2	ZONE 3
METALS	$<0.3\ T'_m$	$0.3 - 0.45\ T'_m$	$>0.45\ T'_m$
OXIDES	$<0.26\ T'_m$	$0.26 - 0.45\ T'_m$	$>0.45\ T'_m$

Figure 2. Structural Zones in Condensates at Various Substrate Temperatures (Movchan and Demchishin).

are not sharp, the structure blending from one morphology to the next with increasing temperature.

For Ni-20Cr alloy based on the above relation, the computed transition temperature between Zone 1 and 2, T_1 is 229°C (502°K) and between Zone 2 and 3, T_2 is 477°C (750°K). Table I lists the transition temperatures, the deposition temperatures and observed grain morphology in the deposits. The morphology of our deposits conform to the characteristic morphology zone model reported by Movchan and Demchishin.[2] From Fig. 3, at 680°C (1200°F), 760°C (1400°F) and 950°C (1740°F) condensation temperatures, typical Zone 3 morphology is exhibited, both the cross-section and surface structure being equiaxed. At a deposition temperature of 427°C (800°F), the morphology was that of Zone 2, equiaxed on surface and columnar grain in cross-section. The grain size for the sample deposited at 427°C is very fine and it is difficult to sense the columnar direction of growth from the photomicrograph although it is more evident in the original sample when viewed in the metallograph. The same problem had occurred in a similar prior investigation on titanium[3] and a special sputter etching technique[7] had been developed, the sample then replicated and photographed in the electron microscope. Unfortunately this set up was not available to the authros at UCLA.

The range of grain size of the deposits varied from 0.5μ to 13μ, as the deposition temperature increased from 470 to 950°C. In the rolled sheets the grain sizes were controlled by the annealing time and temperature Table II shows annealing parameters used. As shown in Fig. 4, the surface of the rolled samples showed an equiaxed grain structure and a slightly elongated grain morphology in cross section. The cross-section photomicrographs are not shown as they are very similar to the surface micrographs.

TABLE I

Characteristic Temperature of
Ni-20Cr for Morphology
Zone Boundaries

CALCULATED

Melting Temperature Tm	Transition Temperatures T_1 (Zone 1 - Zone 2)	T_2 (Zone 2 - Zone 3)
1400°C(1673°K)	229°C(502°K)	477°C(750°K)

EXPERIMENT

Deposition Temperature	Observed Morphology
427°C(700°K)	Columnar (Zone 2)
680°C(923°K)	Equiaxed (Zone 3)
760°C(1033°K)	Equiaxed (Zone 3)
950°C(1223°K)	Equiaxed (Zone 3)

TABLE II

Grain Sizes and Sample Thickness

Deposited Samples

Sample	Substrate Temperature	Grain Size (μ)	Thickness (Inches)
Ni-Cr A	427°C(800°F)	0.5	0.014
Ni-Cr B	680°C(1200°F)	1.8	0.013
Ni-Cr C	760°C(1400°F)	2.6	0.013
Ni-Cr D	950°C(1740°F)	13.0	0.015

Annealing Parameters, Grain Size and Thickness of Rolled Ni-20Cr Sheet

Sample	Annealing Temperature	Annealing Time	Grain Size (μ)	Thickness (Inches)
Ni-Cr-R-1	900°C	10 minutes	1.40	0.008
Ni-Cr-R-2	900°C	20 minutes	2.75	0.008
Ni-Cr-R-3	1000°C	30 minutes	3.90	0.013
Ni-Cr-R-4	1000°C	60 minutes	5.65	0.013
Ni-Cr-R-5	1000°C	120 minutes	7.60	0.013
Ni-Cr-R-6	1000°C	240 minutes	10.40	0.013

DEPOSITION TEMPERATURE AND ZONE MORPHOLOGY

SURFACE

CROSS-SECTION

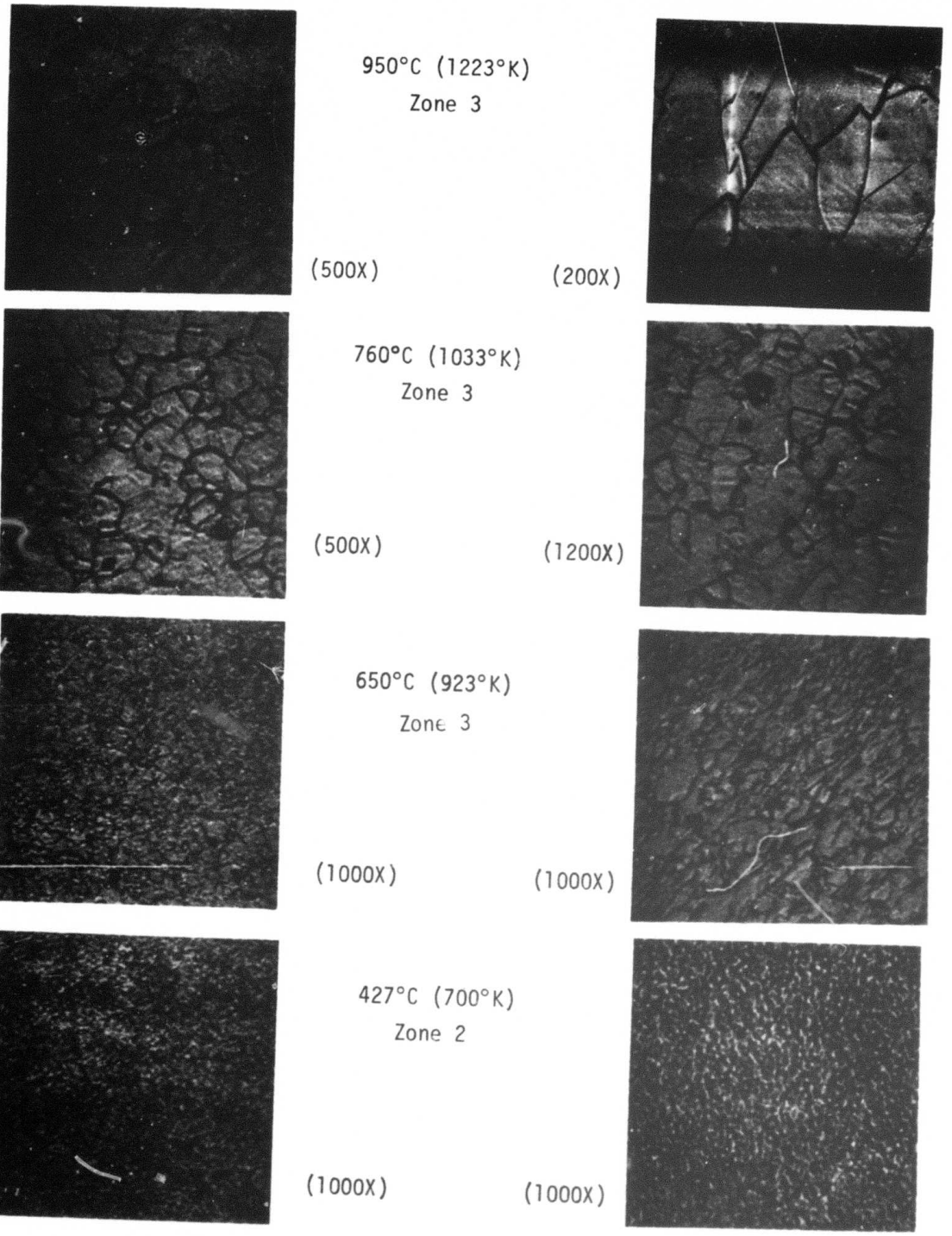

Figure 3: Photomicrographs of Typical Ni-20Cr Deposits at Various Substrate Temperatures.

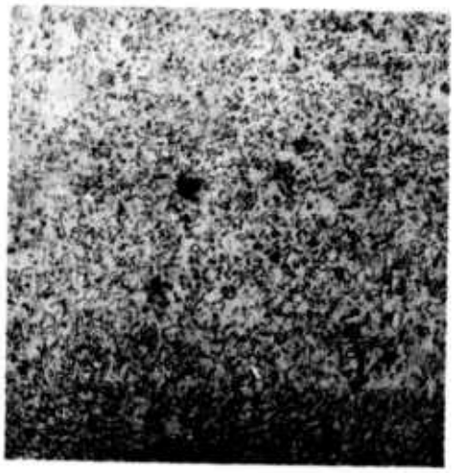

NiCr-R-1 1.4μ (750X)

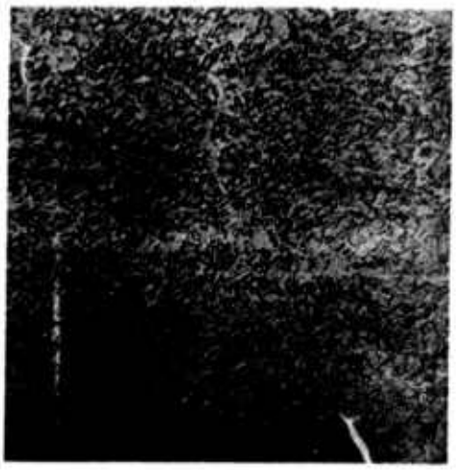

NiCr-R-2 2.75μ (750X)

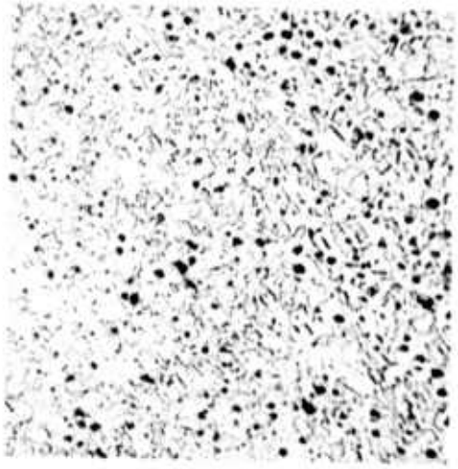

NiCr-R-3 3.90μ (500X)

NiCr-R-4 5.65 (500X)

NiCr-R-5 7.60μ (500X)

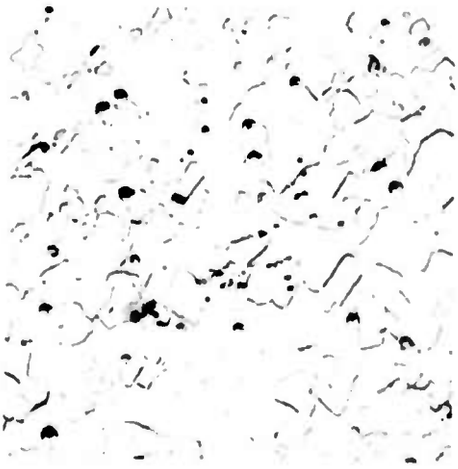

NiCr-R-6 10.40μ (500X)

Figure 4: Surface View of Rolled and Annealed Ni-20Cr Sh-ets Indicating Grainsize.

B. Density

It has been shown previously[3] for the HRPVD process that if the substrate temperature is greater than 0.25Tm, i.e., Zone 2 morphology, the deposit will be fully dense. The present work in consistent with this earlier observation. The density value for both rolled and annealed samples was 8.35 $\pm$ 0.05 g/cm^3. The handbook value of density for Ni-20Cr alloy is 8.4 g/cm^3.

C. Mechanical Properties

1. Tensile Properties

Table III shows the data obtained form the tensile tests for deposited and rolled samples. Yield stress, ultimate tensile strength, percent elongation and percent reduction in area were determined. The deposited samples were tested both at 25°C and 1000°C. The grain size of the deposits varied from 0.5μ to 13μ and corresponding yield stress values at 25°C decreased from 171,000 psi to 48,000 psi. The elongation increased from 6 to 26% and reduction in area from 8 to 27%. Also, from Table III, it is seen that the tensile properties of the deposited material and the wrought material are very similar at equivalent grain sizes. The mechanical properties of wrought Ni-20Cr reported in literature[8] are as follows: Yield stress : 49,300 psi, elongation : 30%, reduction in area : 55%. It is difficult to make a meaningful comparison between this data and our data since the grain size was not reported in ref. (8).

For another comparison, the Hall-Petch relationship was investigated for deposited and wrought material. This was done by plotting yield stress values against the inverse square root of the average grain diameter.[9-11]

TABLE III

Mechanical Properties of Ni-20Cr

Sample	Method of Preparation	Grain Size d(μ)	d-1/2 ($mm^{-1/2}$)	Test Temp. °C	Yield Stress Ksi	Ultimate Tensile Strength Ksi	% Elongation	% Reduction in Area	DPH Hardness (Kg/mm^2)	Bend Ductility ASTM E290-88
Ni-Cr-A	Deposited 427°C	0.50	44.0	25	171.45	174.05	6.25	8.00	179.5	1T 180°
Ni-Cr-B	Deposited 680°C	1.80	23.2	25	107.12	124.31	18.72	19.50	131.5	1T 180°
Ni-Cr-C	Deposited 760°C	2.60	19.7	25	82.12	110.00	21.30	26.10	112.0	1T 180°
Ni-Cr-D	Deposited 950°C	13.00	8.7	25	48.21	76.07	26.43	27.30	80.0	1T 180°
Ni-Cr-A'	Deposited & Stress Relieved(427°C)	0.50	44.0	25	167.80	176.34	7.31	8.54	174.3	1T 180°
Ni-Cr-B'	Deposited & Stress Relieved(680°C)	1.80	23.2	25	105.40	124.15	19.45	20.95	128.0	1T 180°
Ni-Cr-A	Deposited	0.50	44.0	1000	9.14	11.54	53.20	44.15	-	1T 180°
Ni-Cr-B	Deposited	1.80	23.2	1000	5.82	8.46	53.50	41.34	-	1T 180°
Ni-Cr-C	Deposited	2.60	19.7	1000	4.31	6.90	50.00	37.48	-	1T 180°
Ni-Cr-D	Deposited	13.00	8.7	1000	3.62	5.13	25.00	21.63	-	1T 180°
Ni-Cr-R-1	Rolled & Annealed	1.4	28.3	25	129.5	151.6	13.7	11.2	112.5	1T 180°
Ni-Cr-R-2	Rolled & Annealed	2.75	19.1	25	102.30	124.70	27.50	19.8	99.8	1T 180°
Ni-Cr-R-3	Rolled & Annealed	3.90	15.8	25	88.00	105.30	31.20	23.3	96.0	1T 180°
Ni-Cr-R-4	Rolled & Annealed	5.65	13.3	25	68.62	91.67	33.12	26.1	83.4	1T 180°
Ni-Cr-R-5	Rolled & Annealed	7.60	11.5	25	64.57	83.31	36.15	30.9	81.5	1T 180°
Ni-Cr-R-6	Rolled & Annealed	10.40	9.8	25	56.51	81.44	37.80	31.8	78.8	1T 180°

The Hall-Petch relation is

$$\sigma_y = \sigma_y + K_y d^{-1/2}$$

where σ = yield stress

σ_y = Hall-Petch intercept - a measure of stresses necessary to move dislocations in a grain without resistance from grain boundaries.

K_y = Hall-Petch slope - measure of grain boundary resistance to slip at yield.

d = average grain diameter.

Figure 5 shows the Hall-Petch plot for yield stress versus the inverse square root of the average grain diameter showing that both the deposited and wrought material obeys it well. The Hall-Petch Constants were calculated and are listed in Table IV. The possible reasons to explain the difference in the value of these constants between the as-deposited and the wrought material are different levels of impurity content, morphology and/or texture differences in the grain structures as discussed before.

Wilcox et al[9] studied the effect of grain size and temperature on the tensile properties of Ni-20Cr. A plot of yield stress values obtained at different grain sizes is shown in Fig. 5. The grain size variation in their study is from 0.7μ to 17μ which is comparable to the grain size of deposited and wrought specimens used in our study. There is a good agreement in the data obtained by Wilcox et al. and yield stress values obtained in this study. Similar data over a more limited range of grain sizes obtained by Webster[13] also show good agreement with the other data.

Table III also gives tensile properties of deposited samples tested at 1000°C. These yield stress values plotted against inverse square root of grain diameter are shown in Fig. 6. The straight line plot is in agree-

TABLE IV

Hall-Petch Constants for Yield Strength and Hardness

Method of Preparation	Test Temp.	σ_o kg/mm^2	K_y kg/mm$^{3/2}$	H_o kg/mm^2	K_H kg/mm$^{3/2}$
Deposited	25°C	12.64	2.53	55.0	3.0
Deposited	1000°C	1.33	0.12	-	-
Rolled and Annealed	25°C	11.24	2.89	55.4	2.25
Wilcox et al.	25°C	9.83	2.13	-	-

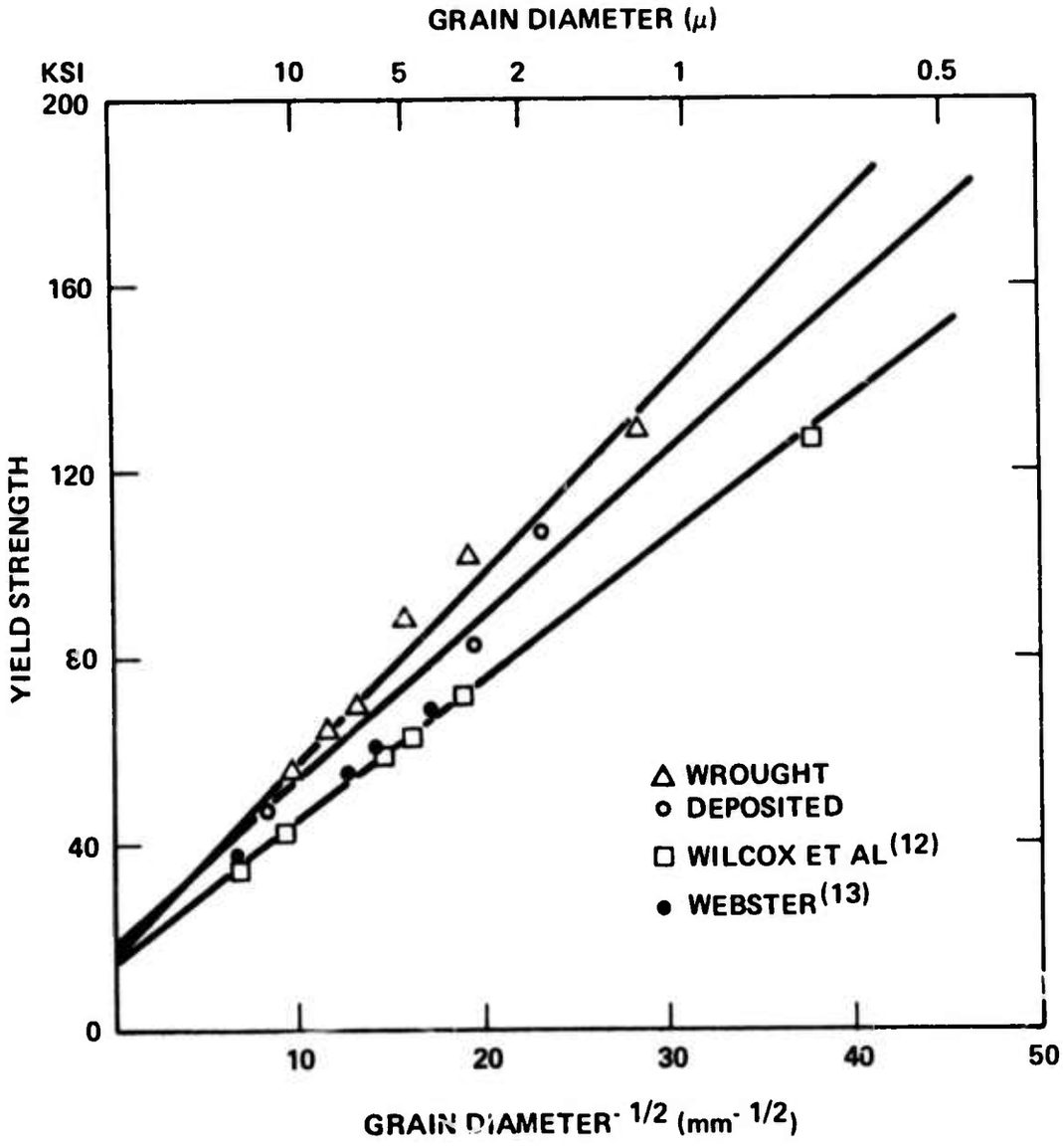

Figure 5. Yield Stress vs Inverse Square Root of Average Grain Diameter for Ni – 20 Cr Alloy at 25 °C.

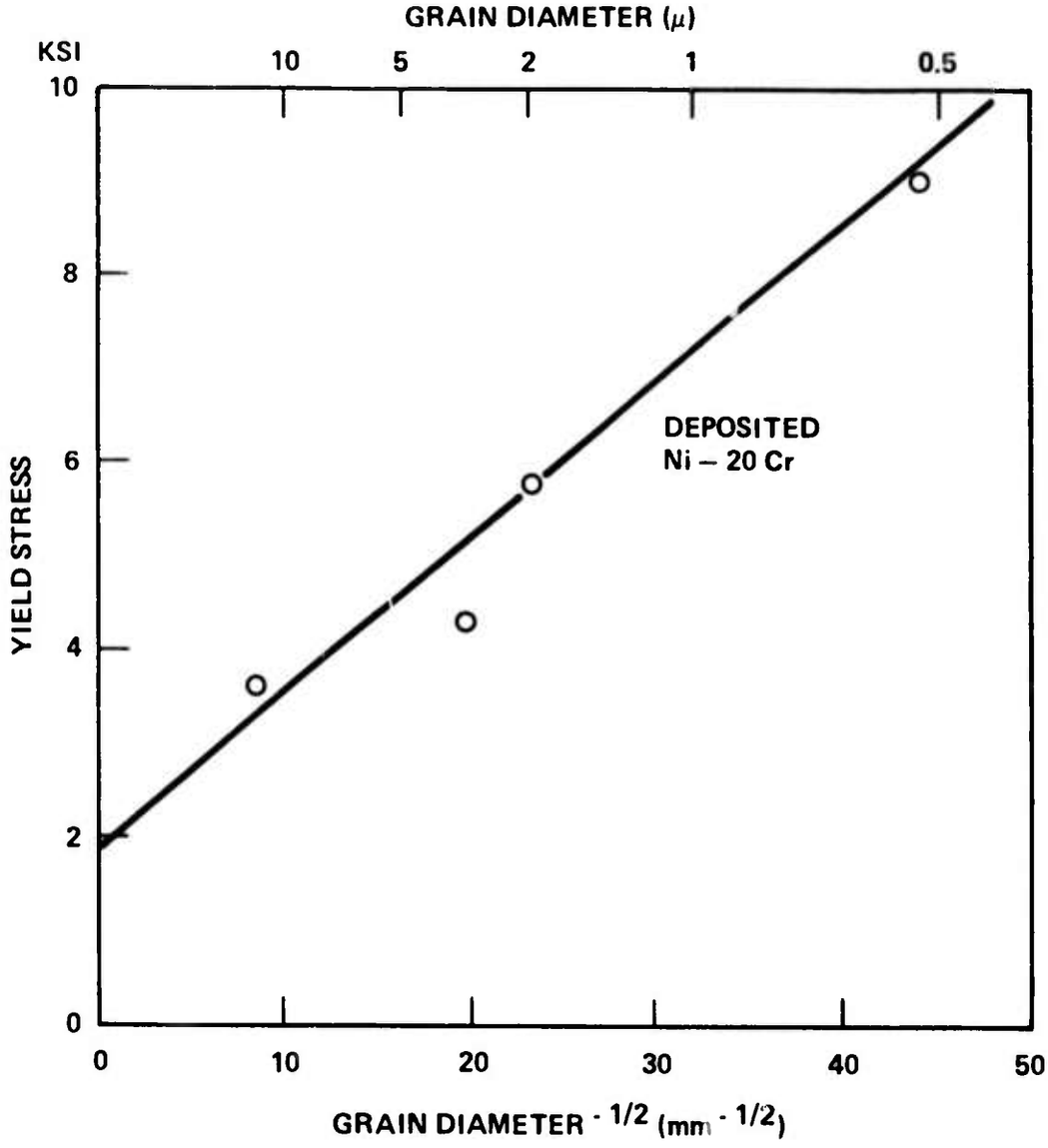

Figure 6. Yield Stress vs Inverse Square Root of Average Grain Diameter for Ni – 20 Cr at 1000 °C.

ment with Hall-Petch relationship. The yield stress varies from 4000 to 9000 psi in the grain size range of 0.5 to 13μ. Comparable yield stress values of 3030 to 4600 psi at 1093°C for grain size range of 0.7μ to 17μ.[12]

To determine whether residual stresses were affecting the mechanical properties, samples of the deposited material were given a stress relief treatment for two hours at 400°C. Testing of the stress relieved samples showed no significant change in tensile properties as shown in Table III.

2. Hardness

Originally, the Hall-Petch relationship was developed to explain the dependence of yield stress on microstructure; however, subsequent work by Armstrong[9] and Bunshah and Armstrong[10] has shown that the same type of equation can be used to explain the relationship of hardness to grain size. This Hall-Petch type relationship is:

$$H = Ho + K_H\, d^{-1/2}$$

where Ho and K_H are experimental constants analogous to the above mentioned Hall-Petch yield stress constants. Table III shows the hardness data for deposited and rolled samples. Table IV gives the Hall-Petch constants H_o and K_H. Figure 7 shows the plot of the hardness vs. the inverse square root of the average grain diameter. It is seen that the hardness of the deposited samples is a few percent higher than the wrought specimen which is in agreement with the slightly larger ductility shown in the wrought material.

3. Bend Ductility

Bend ductility tests showed identical results for all the deposited and rolled samples. All samples were able to withstand a less than 1T/180°

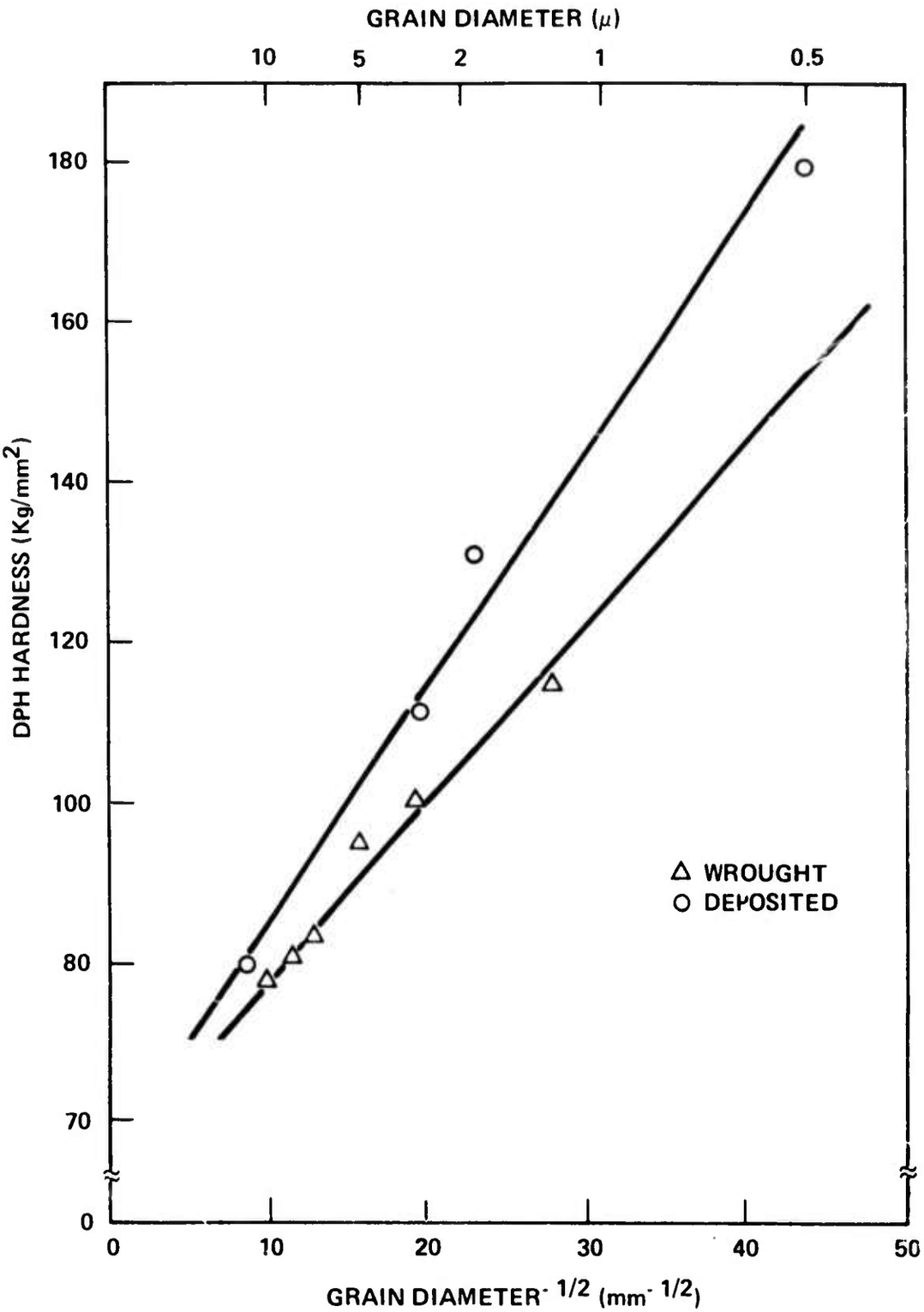

Figure 7. Hardness vs Inverse Square Root of Average Grain for Ni – 20 Cr Alloy.

bend at room temperature. Study of the bent edge in the optical microscope showed no sign of cracking or tearing.

IV. Summary and Conclusions

The high rate physical vapor deposition technique was used to produce Ni-20Cr alloy sheets of full density. The grain size and grain morphology were varied by changing the substrate temperature. Characterization of the deposited material by various mechanical tests showed strength and ductility values comparable to similar purity wrought material. The yield strength and hardness values varied linearly with the inverse square root of the average grain diameter according to the Hall-Petch relationship. It may therefore be concluded that Ni-20Cr alloy sheet produced by HRPVD technique is an engineering material.

V. Acknowledgements

The authors are very grateful to Dr. Pierre Turillon of the International Nickel Co. Research Center for providing us with the Ni-20Cr bars used in this study. They would also like to acknowledge the kind help provided by Dr. Neil Paton of the North American Rockwell Science Center in conducting the elevated temperature tensile tests.

The work was sponsored by ARPA under Grant DAHC-15-70.

References

(1) R. Nimmagadda, A. C. Raghuram, and R. F. Bunshah: J. Vac. Sc. Tech., 9, No. 6, (Nov. - Dec. 1972), 1406.

(2) B. A. Movchan and A.V. Demchishin: Fiz. Metal. Metalloved., 28 No. 4, (1969), 653.

(3) R. F. Bunshah and R. S. Juntz: Metallurgical Transactions, 4, No. 1, (1973), 21.

(4) A. C. Raghuram and R. F. Bunshah: J. Vac. Sc. Tech., 9, No. 6, (1972) 1389.

(5) K. Kennedy: Trans. Int'l. Vac. Met. Conf., Pub. AVS, (1968) 195.

(6) N. F. Kane and R. F. Bunshah.

(7) R. F. Bunshah and H. Olsen, Metallography.

(8) U.S. Department of Commerce, National Bureau of Standards Circular C447, (1943) 351.

(9) R. W. Armstrong, I. Codd, R. Deuthwaite, and N. J. Petch: Phil. Mag., 7 (1962) 45.

(10) R. W. Armstrong: EMG Report No. 2 (June 1968) University of Maryland.

(11) R. F. Bunshah and R. W. Armstrong: Mat. Res. Bull., 4, (1969) 239.

(12) B. A. Wilcox, A. H. Claver and H. B. Hutchinson, NASA CR-72832, (1971) 119.

(13) D. Webster: ASM Transactions Quarterly 62 (1969), 936.

APPENDIX II

SYNTHESIS OF DISPERSION STRENGTHENED ALLOYS BY THE ACTIVATED REACTIVE EVAPORATION FROM A SINGLE ROD-FED ELECTRON BEAM SOURCE

By

R. Nimmagadda
and
R. F. Bunshah

Materials Department
School of Engineering
University of California
Los Angeles, California 90024

ABSTRACT

Oxide dispersion strengthened alloys have better high temperature properties but poorer low temperature strength compared to Ni base super alloys. In comparison to these alloys, dispersion strengthened alloys with titanium carbide dispersed Ni-base alloy matrix have been found to have good low as well as high temperature strength. This investigation was concerned with the synthesis of dispersion strengthened alloys of TiC particles in Ni matrix using the Activated Reactive Evaporation (ARE) process[8]. A Ni-Ti alloy rod was evaporated from an eb source in the presence of C_2H_2, all the vapor species being activated or partially ionized using the ARE process. The deposits were characterized by x-ray diffraction, electron microprobe analysis, microhardness, and transmission electron microscopy of carbon replicas. It was established that Ni-TiC dispersion strengthened alloys were produced by ARE process. Microhardness of the alloys decreased when annealed at high temperatures due to particle coarsening.

Preceding page blank

INTRODUCTION

The dispersion of a finely divided insoluble second phase within a crystalline host material constitutes a powerful technique for the production of high strength composites, called dispersion strengthened alloys. The more common composites of this type are oxide-dispersion strengthened alloys (OD alloys). They show unusually high temperature stability and maintain high levels of strength at high temperatures, which are in the range of 980-1370°C. Unfortunately, OD alloys have not shown, as yet, adequate high strength at low temperatures compared to commercial nickel base superalloys. The strength of OD alloys has been attributed primarily to cold work or stored energy of deformation in the system.[1] Since it is unlikely that the metal matrix is bonded to the oxide in OD systems, bonding forces are not expected to make a large contribution to the strength.[2] It has been suggested that the use of a fine non-oxide dispersoid, which would be bonded to the matrix, would lead to significantly better properties at lower temperatures while maintaining attractive strength properties at a temperature considerably higher than is possible in conventional aging alloys[1]. The refractory carbides, borides, nitrides and other intermetallics are considered suitable dispersoid candidates for such dispersion strengthening. Desirable characteristics of the hard particle would be: low solubility in the matrix, high melting point, high decomposition temperature, high free energy of formation, freedom from crystallographic transformation, and good oxidation resistance.

There are several reasons which force one to consider a group IV or group V monocarbide as a dispersoid for new alloys. These monocarbides

have the highest known melting temperatures of all materials; they have close packed structures; they are only slightly soluble in Ni and Co; and they will deform plastically under stress at very high temperatures.

There are several conventional methods of producing dispersion strengthened alloys[3,4]. One method is to mechanically mix the matrix and the dispersoid particles followed by compaction and sintering. Other methods, stated with reference to OD alloys are internal oxidation, surface oxidation, preferential chemical reduction of mixed oxides, and co-precipitation of matrix and dispersed phase compounds followed by preferential chemical reduction of the matrix metal phase, with consolidation by standard powder metallurgy techniques as a final step. They can be adopted for alloys with other dispersed phases such as carbides, nitrides, etc.

The literature abounds with reports of the difficulties of obtaining optimum dispersion strengthened composites by these processes. The dispersoid particles tend to agglomerate during mixing and then segregate as clusters in the composite. The system titanium carbide dispersed in Nickel has long been of interest, in part because of the relative cheapness, availability and low specific gravity of TiC. The wetting characteristics between Ni and TiC have been found to be favorable also[5]. Murphy and Grant[6] produced Ni-TiC dispersion strengthened alloys by mechanical mixing as well as internal carburization techniques. They observed regions of the alloy devoid of TiC particles and also could only obtain TiC particles of sizes not less than 1000 Å to 5000 Å at 5% TiC. In addition, they encountered the problem of formation of some titanium oxide during

milling and comminution steps. They found that these alloys have significantly higher strengths at low temperatures but poorer creep-rupture properties at high temperatures than OD alloys. Kenton and Grant[7] studied alloys of TiC dispersed in Ni alloy matrix as prospective candidates to show the desirable combination of low and high temperature strength, and good thermal stability upto at least 1090°C. In the as-extruded condition the alloys suffered gross segregation of carbides into stringers. Thermomechanical treatments were necessary to improve the distribution of the carbides. These alloys had better high temperature properties than the alloys containing TiC dispersions in a nickel matrix[6] and compare favorably with OD alloys. These alloys were also found to be stronger than any OD alloys at room temperature.

Thus, we see that TiC dispersed Ni base alloy matrix systems are promising for a combination of good low and high temperature properties. However, the conventional methods of production are laborious and cumbersome; the dispersion of particles is not uniform with particle segregation occurring; oxidation of the powders during blending occurs; and the particle sizes obtained are not fine enough. To alleviate these problems the objective of this investigation is to make a feasibility study of synthesizing Ni-TiC dispersion strengthened alloys by the Activated Reactive Evaporation[8] of alloys. In this process, a Ni-Ti alloy is evaporated using a rod-fed electron beam source and the vapors are reacted with C_2H_2 molecules introduced into the reaction zone to form the compound, the reaction being promoted by activation and/or ionization of the metal vapor atoms and C_2H_2 gas species by the secondary electrons drawn from the plasma sheath above

the molten pool into the reaction zone by the probe biased to a small positive dc voltage as shown in Fig. 1.

EXPERIMENTAL PROCEDURE

A Ni-Ti alloy rod was evaporated by electron beam heating in the experimental arrangement shown in Fig. 1 as described by Bunshah and Raghuram[8]. The reactive gas, C_2H_2, was introduced into the system after steady state conditions of evaporation were attained[9], i.e. the vapor composition was the same as that of the evaporant rod. The deposits were made under the experimental conditions as given in Table I. It was expected that Ti reacts with the gaseous species and forms TiC particles and Ni deposits as a pure metal matrix because the free energy of formation for nickel carbide Ni_3C is unfavorable ($\Delta G°_{900}$ = + 8.2 Kcal/mole).[10] One deposit of Ni-Ti alloy (C-1) was made in the absence of C_2H_2 to compare with Ni-TiC deposits.

The deposits were analyzed by x-ray diffraction to ascertain the phases present. The microhardnesses of the deposits were measured using a Micromet microhardness tester with a Knoop indentor and 50 g load. For microstructural examination, some deposits were electropolished in a solution of 2 H_2SO_4, 1 HCℓ and 7 methyl alcohol. Carbon replicas of these electropolished samples were made and observed with a Hitachi transmission electron microscope. Deposits were also analyzed with an electron microprobe analyzer after mounting the samples and giving them a metallographic polish, the final step being carried out with 0.3 μm alumina powder.

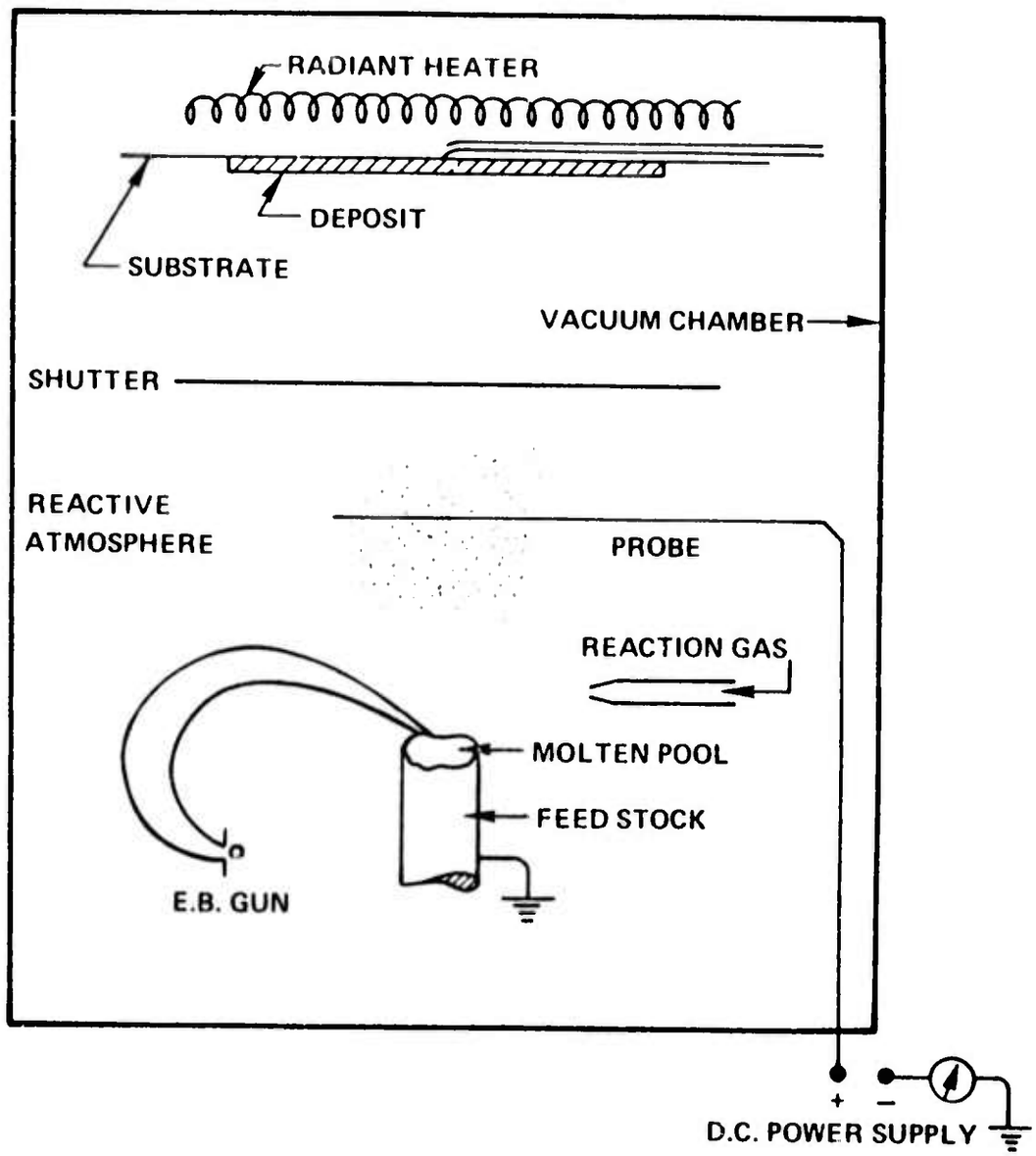

Figure 1. Schematic of the Experimental Arrangement for the Activated Reactive Evaporation Process.

RESULTS AND DISCUSSION

The microprobe, x-ray diffraction, and microhardness results of the deposits are given in Table I. The deposits C-1, C-10, C-20, C-21, and C-11 have the same amount of Ti. The higher hardness of the carbide deposits compared to the alloy deposit is therefore attributed to dispersion strengthening due to TiC formation. The carbide deposit C-5 has very high hardness (1000 KHN) because of the large amount of TiC present. X-ray diffraction patterns of the carbide deposits did not show TiC peaks except that of C-5 which showed strong TiC peaks. The absence of TiC peaks in the diffraction patterns of these carbide deposits C-10, C-20, C-21, and C-11 could be attributable to the low detection sensitivity of the x-ray diffraction technique in this case due to the following reasons; 1) Small amount of TiC, 2) fine dispersion of the carbide, and 3) high background in the diffraction pattern due to the fluorescence produced by the interaction of copper radiation with Ni matrix.

When carbon replicas of the carbide deposits were observed with the transmission electron microscope, TiC particles were observed only in the replicas of the C-5 deposit and the micrograph is shown in Fig. 2. The average particle size of TiC has been estimated to be ~560 Å and the mean spacing between the particles is ~2500 Å. The replicas from other Ni-TiC samples did not show any TiC particles. This is possibly due to a very small amount of TiC and hence a very small particle size (<200 Å) which is the detection limit for the replica technique used. Movchan, et al.[11] observed a correlation between particle size and the percent of dispersoid present in Fe-NbC alloys. They observed that the NbC particle size increased from 150 to 900 Å when the NbC content in Fe

TABLE I

Experimental Parameters for the Formation of Dispersion Strengthened Deposits of TiC Particles in Ni matrix by Evaporating Ni-Ti Alloy in the Presence of C_2H_2 and Their Characteristics

Run Number	Evaporation Rate g/min.	C_2H_2 gas Pressure torr	Temperature of Deposition °C	Probe		Composition of Deposit wt. %	Whether X-ray Diffract. Pattern Showed TiC Peaks	Microhardness KHN Kg/mm^2
				Voltage Volts	Current Amps.			
C-1 Alloy deposit in the absence of C_2H_2	0.71	-	638	-	-	Ni-0.2 Ti	-	138
C-10	0.72	$2\text{-}3 \times 10^{-3}$	627	100-110	2-4	Ni-0.2 TiC	No	312
C-20	0.32	$7\text{-}8 \times 10^{-4}$	627	65-120	0.2-0.4	Ni-0.2 TiC	No	344
C-21	0.64	$7\text{-}8 \times 10^{-4}$	638	85	0.5-0.7	Ni-0.2 TiC	No	365
C-11	0.91	$3\text{-}4 \times 10^{-4}$	627	55-70	1-2	Ni-0.2 TiC	No	367
C-5	1.45	$8\text{-}9 \times 10^{-4}$	638	25	2-4	Ni-18 TiC	Yes	1000

Figure 2. Transmission Electron Micrograph of Carbon Replica of Ni-TiC Deposit (C-5) Showing TiC Particle Dispersion in Ni Matrix (33000 X).

matrix increased from 1 to 10%. They could observe the NbC particles by electron microscope only after extracting the particles by chemical dissolution of the condensate.

Samples from high hardness deposit (C-5) were annealed in vacuum at various temperatures for 2 hours and microhardness was measured. The results are given in Table II. It can be seen that the hardness drops as the annealing temperature is increased. This is due to the familiar phenomenon of dispersoid particle coarsening.

CONCLUSIONS

This study shows that dispersion strengthened alloys of TiC in Ni matrix can be produced by Activated Reactive Evaporation from a single rod-fed electron beam source. This can be further extended to produce dispersion strengthened alloys with TiC particle dispersion in solid solution strengthened matrices, such as Ni and Co base alloys for a combination of good high and low temperature strength. Such deposits could be produced as free standing shapes or coatings for various applications.

ACKNOWLEDGMENTS

This research was supported by the Advanced Research Projects Agency under Grant No. DAHL 15-70-6-15.

TABLE II

The Variation of Microhardness of Ni-TiC Deposit (C-5)
After 2 Hrs. Vacuum Annealing at Temperature

Annealing Temperature °C	Microhardness KHN Kg/mm^2
As Deposited	1000
700	870
800	785
850	705
900	595
950	490
1000	340

REFERENCES

1. N. J. Grant, "The Strengthening of Metals," edited by D. Peckner (Reinhold Publishing Co., New York, 1964).
2. B. E. Edelson and W. M. Baldwin, Jr., ASM Trans. Quart. 55, 230 (1962).
3. R. F. Bunshah and C. G. Goetzel, "A Survey of Dispersion Strengthening of Metals and Alloys," WADC Tech. Rept. 59-414 (March 1960).
4. C. G. Goetzel and R. F. Bunshah, "Powder Metallurgy," Proc. Int. Conf., sponsored by Metal Powder Industries and Met. Soc. AIME, held in New York (June 13-17, 1960), Interscience Publishers, New York.
5. J. Gurland, Trans. AIME 215, 601 (1959).
6. R. J. Murphy and N. J. Grant, Trans. ASM 60, 29 (1967).
7. D. J. Kenton and N. J. Grant, Fine Particles-Second International Conference, 308 (1973).
8. R. F. Bunshah and A. C. Raghuram, J. Vac. Sci. Technol. 9, 1385 (1972).
9. R. Nimmagadda, A. C. Raghuram and R. F. Bunshah, J. Vac. Sci. Technol. 9, 1406 (1972).
10. L. S. Darken and R. W. Gurry, Physical Chemistry of Metals (McGraw-Hill, New York, 1953) pp. 361-364.
11. B. A. Movchan, A. V. Demchishin and L. D. Kooluck, J. Vac. Sci. Technol. 11, 869 (1974).

APPENDIX III

List of Publications from this Grant

1. Chow, R. and Bunshah, R. F., "Model for Calculating the Deposit Temperature in High Rate Physical Vapor Deposition Process," J. Vac. Sci. Tech., 8:73, Nov./Dec. 1971.

2. Nimmagadda, R. and Bunshah, R. F., "Temperature and Thickness Distribution on the Substrate During High Rate Physical Vapor Deposition of Materials," J. Vac. Sci. Tech. 8:85, Nov./Dec. 1972.

3. Bunshah, R. F. and Raghuram, A. C., "Activated Reactive Evaporation Process for High Rate Deposition of Compounds," J. Vac. Sci. Tech., 9:1385-88, Nov./Dec. 1972.

4. Raghuram, A. C. and Bunshah, R. F., "The Effect of Substrate Temperature on the Structure of Titanium Carbide Deposited by Activated Reactive Evaporation," J. Vac. Sci. Tech., 9:1389-94, Nov./Dec. 1972.

5. Nimmagadda, R., Raghuram, A. C. and Bunshah, R. F., "Preparation of Alloy Deposits by Continuous Electron Beam Evaporation from a Single Rod-Fed Source," J. Vac. Sci. Tech., 9:1406-12, Nov./Dec. 1972.

6. Raghuram, A. C., Nimmagadda, R., Bunshah, R. F. and Wagner, C. N. J., "Structure and Microhardness Relationships in Ti, Zr and Hf-3Zr Carbide Deposits Synthesized by Activated Reactive Evaporation," Thin Solid Films, 20:187-199, 1974.

7. Bunshah, R. F., "High Rate Evaporation/Deposition Processes of Metals, Alloys and Ceramics for Vacuum Metallurgical Applications," J. Vac. Sci. Tech., 11:814, 1974.

8. Bunshah, R. F., "Structure/Property Relationships in Evaporated Thick Films and Bulk Coatings," J. Vac. Sci. Tech., 11:633, 1974.

9. Bunshah, R. F., "High Rate Physical Vapor Deposition Processes," Proc. 16th Annual Conf., Soc. Vac. Coaters, 1973, p. 5.

10. Bunshah, R. F., "Physical Vapor Deposition of Metals, Alloys, and Ceramics," The Banaras Metallurgist, V. 5, 1973, p. 207.

11. Bunshah, R. F., "Reactive Evaporation," Science and Technology of Surface Coatings, Academic Press, 1974.

12. Kane, N. F. and Bunshah, R. F., "Effect of Substrate Temperature on Ni Sheets produced by HRPVD and Comparison with Rolled Ni Sheets," Proc. 4th Int'l. Vac. Met. Conf., Iron and Steel Institute, Japan, 1974.

13. Beale, H. A., Weiler, F., and Bunshah, R. F., "Evaporation Variables in Gas Scattering Plating Process," Proc. 4th Int'l. Vac. Met. Conf., Iron and Steel Institute, Japan, 1974.

Appendix III (Cont.)

14. Bunshah, R. F., "Physical Vapor Deposition of Metals, Alloys and Ceramics," Proc. 4th Int'l. Vac. Met. Conf., Iron and Steel Institute, Japan, 1974.

15. Agarwal, N., Kane, N., and Bunshah, R. F., "Structure and Property Relations of Ni-20Cr Produced by High Rate Physical Vapor Deposition," J. Vac. Sci. Tech.

16. Bunshah, R. F., "High Rate Physical Vapor Deposition of Compounds by Activated Reactive Evaporation", U.S. Patent No. 3,791,852, February 12, 1974.